

Facile Oxidation of Leucomethylene Blue and Dihydroflavins by Artemisinins: Relationship with Flavoenzyme Function and Antimalarial Mechanism of Action

Richard K. Haynes,^{*,[a]} Wing-Chi Chan,^[a] Ho-Ning Wong,^[a] Ka-Yan Li,^[a] Wai-Keung Wu,^[a] Kit-Man Fan,^[a] Herman H. Y. Sung,^[a] Ian D. Williams,^[a] Davide Prosperi,^[c] Sergio Melato,^[b] Paolo Coghi,^[b] and Diego Monti^{*,[b]}

Dedicated to the memory of Prof. Athelstan L. J. Beckwith (R.K.H.) and Prof. Mario Ghione (D.M.), who introduced the importance of research in malaria.

The antimalarial drug methylene blue (MB) affects the redox behaviour of parasite flavin-dependent disulfide reductases such as glutathione reductase (GR) that control oxidative stress in the malaria parasite. The reduced flavin adenine dinucleotide cofactor FADH₂ initiates reduction to leucomethylene blue (LMB), which is oxidised by oxygen to generate reactive oxygen species (ROS) and MB. MB then acts as a subversive substrate for NADPH normally required to regenerate FADH₂ for enzyme function. The synergism between MB and the peroxidic antimalarial artemisinin derivative artesunate suggests that artemisinins have a complementary mode of action. We find that artemisinins are transformed by LMB generated from MB and ascorbic acid (AA) or *N*-benzylidihydronicotinamide (BNAH) in situ in aqueous buffer at physiological pH into single electron transfer (SET) rearrangement products or two-electron reduction products, the latter of which dominates with BNAH. Neither AA nor BNAH alone affects the artemisinins. The AA–MB SET reactions are enhanced under aerobic conditions, and the major products obtained here are structurally closely related to one such product already reported to form in an intracellular medium. A ketyl arising via SET with the artemisinin is invoked to explain their formation. Dihydroflavins generated from riboflavin (RF) and FAD by pretreatment with sodium dithionite are rapidly oxidised by artemisinin to the parent flavins. When catalytic amounts of RF, FAD, and other flavins are reduced in situ by excess BNAH or NAD(P)H in the presence of the artemisinins in the aqueous buffer, they are rapidly oxidised to the parent flavins with concomitant formation of two-electron reduction products from the artemisinins; regeneration of the reduced flavin by excess reductant maintains a cat-

alytic cycle until the artemisinin is consumed. In preliminary experiments, we show that NADPH consumption in yeast GR with redox behaviour similar to that of parasite GR is enhanced by artemisinins, especially under aerobic conditions. Recombinant human GR is not affected. Artemisinins thus may act as antimalarial drugs by perturbing the redox balance within the malaria parasite, both by oxidising FADH₂ in parasite GR or other parasite flavoenzymes, and by initiating autoxidation of the dihydroflavin by oxygen with generation of ROS. Reduction of the artemisinin is proposed to occur via hydride transfer from LMB or the dihydroflavin to O1 of the peroxide. This hitherto unrecorded reactivity profile conforms with known structure–activity relationships of artemisinins, is consistent with their known ability to generate ROS in vivo, and explains the synergism between artemisinins and redox-active antimalarial drugs such as MB and doxorubicin. As the artemisinins appear to be relatively inert towards human GR, a putative model that accounts for the selective potency of artemisinins towards the malaria parasite also becomes apparent. Decisively, ferrous iron or carbon-centered free radicals cannot be involved, and the reactivity described herein reconciles disparate observations that are incompatible with the ferrous iron–carbon radical hypothesis for antimalarial mechanism of action. Finally, the urgent enquiry into the emerging resistance of the malaria parasite to artemisinins may now in one part address the possibilities either of structural changes taking place in parasite flavoenzymes that render the flavin cofactor less accessible to artemisinins or of an enhancement in the ability to use intracellular human disulfide reductases required for maintenance of parasite redox balance.

[a] Prof. Dr. R. K. Haynes, W.-C. Chan, Dr. H.-N. Wong, K.-Y. Li, W.-K. Wu, K.-M. Fan, Dr. H. H. Y. Sung, Prof. Dr. I. D. Williams
Department of Chemistry, Institute of Molecular Technology for Drug Discovery and Synthesis, The Hong Kong University of Science and Technology, Clear Water Bay, Kowloon, Hong Kong (P.R. China)
Fax: (+852) 2358-1594
E-mail: haynes@ust.hk

[b] Dr. S. Melato, Dr. P. Coghi, Prof. Dr. D. Monti
Department of Organic and Industrial Chemistry
CNR-ISTM, Via G. Venezian 21, 20133 Milan (Italy)
Fax: (+39) 02-50314072
E-mail: diego.monti@istm.cnr.it

[c] Dr. D. Prosperi
Department of Biotechnology and Bioscience
Piazza della Scienza 2, 20133 Milan (Italy)

Supporting information for this article is available on the WWW under <http://dx.doi.org/10.1002/cmdc.201000225>.

Introduction

The discovery of artemisinin **1**^[1] has led to the worldwide use of **1** and its derivatives dihydroartemisinin (DHA) **2**, artemether **3**, and artesunate **4** (Figure 1) in combination therapies with other drugs against malaria.^[2] Artemisone **5** is a new derivative

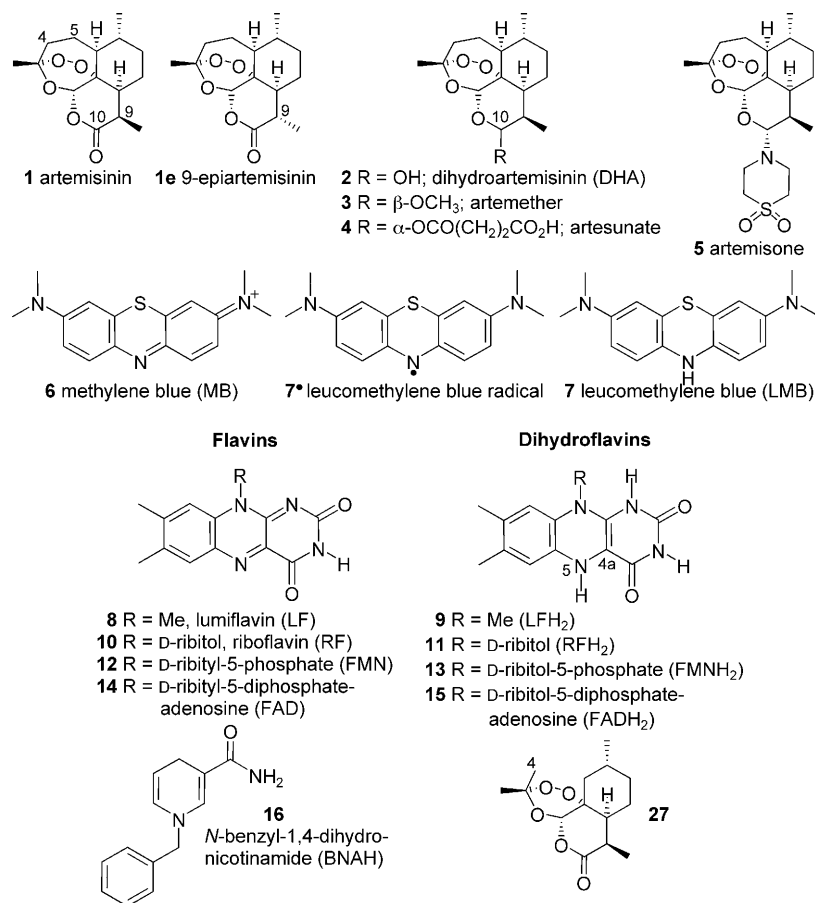


Figure 1. Artemisinins and redox-active substrates discussed in this study.

that shows enhanced efficacy in clinical trials.^[3] The unusual nature of the peroxide pharmacophore poses a formidable challenge to understanding the molecular mechanism of these remarkable drugs. It is universally considered that any of ferrous iron, ferrous hemoglobin [Hb-Fe^{II}], or ferrous heme [heme-Fe^{II}] activate the peroxide^[4] via Fenton chemistry to provide carbon radicals as the nominated cytotoxic agents.^[5,6] For heme-Fe^{II}, the C radicals may alkylate the heme nucleus to provide adducts that are also assumed to discharge the potent activities of the parent artemisinin.^[7] However, artemisinins, especially those bearing an amino group at C10,^[8] are not easily decomposed by Fe^{II} in aqueous medium.^[8,9] Artemisinins susceptible to decomposition by Hb- or heme-Fe^{II}, such as artemisinin **1** itself, display enhanced activities against parasites cultured under carbon monoxide, a reagent that passivates Hb- and heme-Fe^{II} by virtue of the formation of CO-Hb-Fe^{II} and CO-heme-Fe^{II} complexes that block reaction of the Fe^{II}

ion with the artemisinin peroxide.^[10] Thus, the reaction with heme in the malaria parasite represents a competing degradation that results in attrition of efficacy. A consistent correlation between antimalarial activity and reactivity towards Fe^{II} in its various forms does not exist.^[9,10] In general, the ongoing debate over the involvement of iron^[6] is due in large part to

the rather differing outcomes of reactions usually conducted with stoichiometric or excess amounts of iron-based reagents in organic or aqueous solvents, especially those involving heme-Fe^{II} generated under highly reducing conditions. As such, few of these reactions can be termed 'biomimetic'.^[8-11] Artemisinins, like the sesquiterpene thapsigargin (TG), are reported to inhibit the parasite endoplasmic reticulum transmembrane calcium pump PfATP6, a process that is also posited to require ferrous iron.^[12] It is unclear how structurally diverse peroxides that possess antimalarial activities at nanomolar levels in vitro inhibit PfATP6; binding into the TG cleft appears not to be an option.^[13]

Artemisinins enhance oxidative stress in parasitised erythrocytes^[14] and display synergism with doxorubicin, a drug that also increases oxidative stress.^[15] Antioxidant gene expression in tumor cells inversely correlates with the IC₅₀ values for artesunate **4**, indicating that oxidative stress plays a role in the pronounced cytotoxicities of artemisinins against tumor cells.^[16]

Rapid generation of reactive oxygen species (ROS) and lipid peroxidation occur in neuronal cell cultures upon application of artemisinin.^[17] The in vivo pathway to ROS has not been established, but the peroxide bridge is clearly required.^[18]

Like artemisinins, methylene blue (MB) **6** possesses potent activity in vitro against *Plasmodium falciparum*.^[19] MB is equipotent with artesunate when each is used in combination therapy with amodiaquine against malaria in a clinical setting.^[20] MB has a synergistic action with artemisinins, with FIC₅₀ values substantially less than unity.^[21] This is significant given the likely targets of MB: the parasite flavoenzymes glutathione reductase (GR) and thioredoxin reductase (TrxR).^[22,23,24] It is cleverly deduced that incipient reduction of MB by the reduced GR cofactor FADH₂ **15** (Figure 1) generates leucomethylene blue (LMB) **7**, whose oxidation by oxygen regenerates MB with concomitant formation of ROS.^[24] NADPH, otherwise required for reduction of FAD to FADH₂, is then hijacked as it becomes en-

gaged in a futile cycle involving reduction of MB to LMB. With this interference to disulfide reductase function, the capacity of the parasite to counter the enhanced oxidative stress is fatally impaired.

Flavin analogues^[25] and riboflavin (RF) **10**^[26] itself possess appreciable antimalarial activities. The antimalarial activity of RF is ascribed to a redox cycle involving reduction of parasite methemoglobin by the reduced riboflavin (RFH₂) **11** generated from RF and NAD(P)H. Thus, RF also acts as a subversive substrate by consuming NAD(P)H. However, RFH₂ is rapidly converted by oxygen into the corresponding 4a-hydroperoxide^[27] that reverts to riboflavin upon expulsion of hydroperoxide. In this way, *oxidation of dihydroflavins by oxygen generates ROS*;^[27,28] this is significant in relation to the results with glutathione reductase described below.

Acquiring an understanding of the mechanism of action of artemisinins is assuming much greater importance now in the face of the increasing tolerance of the malaria parasite to artemisinins, that is ominously occurring in a region of the world where resistance to chloroquine was first reported.^[29] Development of full-blown resistance will effectively mean an end to efforts to control malaria by chemotherapeutic means.^[4,30] Given that our previous work points to the unlikelihood of C radicals or of heme in triggering the antimalarial activity of artemisinins,^[8–10] we adopt a rather different approach to a consideration of the molecular mechanism. Because, as pointed out above, artemisinins generate ROS, and behave synergistically with drugs such as methylene blue and doxorubicin, which are themselves redox active, we posit that they act as electron acceptors, and thereby are likely to interfere with redox-active cofactors.^[9] Iron is *not* considered to be essential, although as we have pointed out previously, its presence certainly will play a role in modulating oxidative stress^[31] within the malaria parasite that is *independent* of any reaction with artemisinins.^[9] Therefore, an examination of the interaction of artemisinins with redox-active, biologically pertinent substrates is now addressed. We commence with an examination of the reduced conjugates of each of MB and the biologically significant flavins, the structures of which are shown in Figure 1. The conjugates are generated catalytically from MB and the flavins in neutral aqueous buffer, as they would be in the biological milieu, in the *presence of the artemisinin and biological reductants* L-(+)-ascorbic acid (AA) (for MB), the NADH model compound *N*-benzyl-1,4-dihydropyridinamide (BNAH) **16**, and each of NADH and NADPH. The reductants alone do not affect the artemisinins. Ferrous iron is not required, and C radicals held to trigger the parasitocidal process cannot be involved.

Results

Leucomethylene blue

The reduction of MB **6** to LMB **7** by dithionite in pH 7.4 aqueous buffer was monitored by disappearance of the absorption at λ 654 nm.^[32,33] Treatment with artemisinin **1** resulted in oxidation of LMB to MB (Figure 2). Dithionite alone has no effect on artemisinin under these conditions. The lipid-soluble LMB

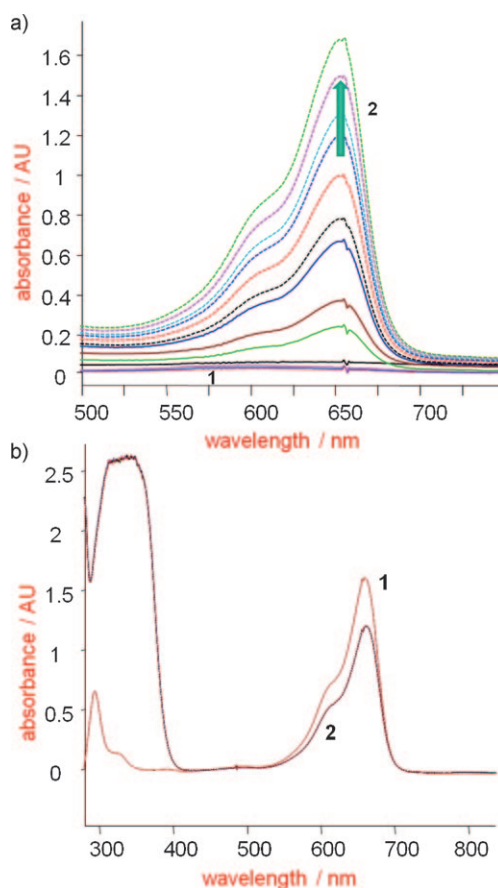
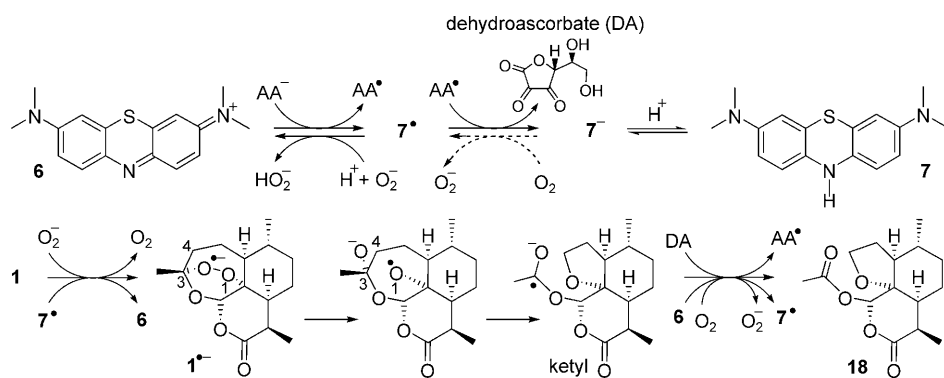


Figure 2. a) Reduction of methylene blue and re-oxidation by artemisinin: 1. MB (0.015 mmol) in pH 7.4 phosphate buffer under argon treated with sodium dithionite (0.14 mmol) is converted into LMB **7** as gauged by the disappearance of absorption due to MB at λ_{max} 654 nm. 2. Artemisinin **1** (1.7×10^{-3} mmol in MeCN) added to **7** (3.1×10^{-3} mmol) in the MeCN/aqueous pH 7.4 buffer solution under argon results in re-oxidation to MB, as gauged by the reappearance of absorption at λ_{max} 654 nm; spectra were recorded at ~ 1 min intervals from 0–10 min when oxidation to MB was complete. b) Partial reduction of MB by NADH: 1. Spectrum obtained from a buffer solution containing 7.8×10^{-5} mmol MB; at λ 663 nm, absorption is 1.6. 2. Treatment of the solution with 1.5×10^{-3} mmol NADH gives a spectrum with an absorption maximum of 1.18 at λ 663 nm, corresponding to a reduction of $\sim 28\%$ of the MB to LMB.

was extracted into dichloromethane. Treatment of this solution with **1** also resulted in oxidation of LMB, although in the non-polar solvent, the reaction was slower (Supporting Information). To both mimic biological redox cycling and to facilitate isolation of products, agents that generate LMB from MB in situ in the presence of **1** were examined. Ascorbic acid (AA) at neutral pH reduces MB via single-electron transfer (SET) to give the radical **7'** and then LMB **7** (Scheme 1).^[32,33] If oxygen is present, oxidation of LMB to MB via **7'** takes place. The resulting superoxide is converted into hydroperoxide (HOO⁻) as it oxidises AA to the ascorbyl radical.^[34] The ascorbyl radical does not react with oxygen, but disproportionates to dehydroascorbic acid (DA) and AA. As artemisinin **1** in 1:1 MeCN/aqueous pH 7.4 buffer is unaffected by excess AA, or a mixture of AA and DA, the MB–AA system is eminently suited for establishing whether artemisinins react with LMB **7** or its radical precursor



Scheme 1. SET between artemisinin **1** and MB-AA. **1** is converted by SET from **7•** into peroxy radical anion **1•-**, which rearranges via an O1 radical to the ketyl by insertion into the C3–C4 bond. The ketyl is oxidised to the carbonyl **18**. Leucomethylene blue anion **7•-** or LMB **7** is intercepted by artemisinin in heterolytic processes (see Scheme 2), and accordingly, oxidation of **7•** to **7•-** by oxygen is expected to be a minor pathway. The greater conversion of **1** with MB-AA under air (Table 1) indicates the importance of the oxygen-initiated radical pathways; this may also implicate superoxide in a Haber–Weiss process for recycling of **1** into **1•-** (see reference [9]). The consequence will be an enhanced oxidative flux that arises from recycling of MB via the radical and of oxidation of the ketyl.

7•. Treatment of MB with a 10-fold excess of AA under argon resulted in ~20% reduction of the MB as established by UV spectroscopy. Addition of MB (0.2 equiv) to artemisinin **1** (1.0 equiv) and AA (4 equiv) under air in the dark over 24 h gave a mixture containing unchanged artemisinin **1**, 2-deoxyartemisinin **17**, and the furanoacetate **18** (Figure 4 below and Table 1). Dihydroartemisinin (DHA) **2** provided a mixture containing **2** and the products 2-deoxyDHA **19**, the tricarbonyl compound **20**, and the furanodicarbonyl compound **21**. Under argon, the conversion of each of **1** and **2** was markedly lower. Each of artemether **3**, artesunate **4**, and artemisone **5** with MB-AA under air gave related products.

NAD(P)H and models such as *N*-benzyl-1,4-dihydronicotinamide (BNAH) **16** reduce MB, but unlike AA, SET is not involved.^[22,35] Treatment of MB with NADH (20 equiv) in MeCN/aqueous buffer (pH 7.4) under argon gave ~28% of LMB (Figure 2). Whilst artemisinin **1** (1 equiv) was unaffected by BNAH (4 equiv), addition of MB (0.2 equiv) in the dark after 24 h returned **1**, 2-deoxyartemisinin **17**, and the ring-opened precursor **25**. With DHA **2**, the control reaction with BNAH (4 equiv) in MeCN/pH 7.4 buffer had an unexpected outcome in providing the peroxyhemiacetal **26**, a compound otherwise obtained by thermal treatment of DHA.^[36] In the absence of BNAH, there is no rearrangement of DHA. With MB-BNAH under air, DHA **2** gave 2-deoxyDHA **19** and the previously unreported 9-epideoxyDHA **19e**. The structure of **19e** was unambiguously determined by X-ray crystallography (see Figure 7 below). Under argon, **19e** was the only product formed. This was also obtained by treatment of 2-deoxyDHA **19** with BNAH in MeCN/buffer.

With the exception of **19e**, the products shown in Figure 4 are identical to those obtained from ferrous iron reactions.^[5,8,9,11] These are subdivided into two classes: those arising via formal two-electron reduction and those arising via SET. Whereas the MB-AA system provides both types, the MB-BNAH system predominantly gives the reduction products.

Dihydroflavins

Lumiflavine (LF) **8** and riboflavin (RF) **10** are used as models to delineate the function of flavin adenine mononucleotide (FMN) and flavin adenine dinucleotide (FAD) in flavoenzymes during reduction by NAD(P)H.^[37,38] Reduction of RF or FAD in 1:1 MeCN/aqueous pH 7.4 buffer by sodium dithionite under argon generated the dihydroflavins. Addition of artemisinin **1** resulted in rapid oxidation. This is illustrated in Figure 3 for the RF-RFH₂ system. Treatment of LF or RF with NADH (10 equiv) in MeCN/pH 7.4 buffer under argon

Table 1. Yields of products from methylene blue–leucomethylene blue redox-mediated decomposition of artemisinsins 1–5.

Artemisinin: R (Figure 1) Method ^[a]	Artemisinin remaining and product yields [%] ^[b] (Figure 4)
1: artemisinin R=O	1. MB-AA, air 1: 30, 17 : 12, 18 : 41
	2. MB-AA, Ar 1: 40, 17 : 14, 18 : 38
	3. MB-BNAH, air 1: 42, 17 : 17, 25 : 32
	4. MB-BNAH, Ar 1: 32, 17 : 20, 25 : 27
2: DHA R=OH	1. MB-AA, air 2: 3, 19 : 17, 20 : 6, 21 : 26
	2. MB-AA, Ar 2: 91, 20 : 26, 21 : 19
	3. MB-BNAH, air 2: 0, 19 : 16, 19e : 47
	4. MB-BNAH, Ar 2: 0, 19e : 63
3: artemether R=OCH ₃	1. MB-AA, air 3: 3, 20 : 4, 21 : 3, 22 : 59, 23 : 17
	2. MB-AA, Ar 3: 84, 22 : 67, 23 : 26
4: artesunate R=OOC(CH ₂) ₂ COOH	1. MB-AA, air 4: 15, 24 : 65
	2. MB-AA, Ar 4: 1, 24 : 63
5: artemisone R=4'-(S,S)-dioxothiomorpholin-1'-yl	1. MB-AA, air 5: 24, 20 : 11, 21 : 27
	2. MB-AA, Ar 5: 28, 20 : 13, 21 : 26

[a] Reactions performed in 1:1 MeCN/aqueous buffer (pH 7.4): 1. artemisinin (1.0 equiv, 0.34 mmol), methylene blue (MB, 0.2 equiv), ascorbic acid (AA, 4.0 equiv), air, 20 °C, 24 h; 2. as for 1, under argon; 3. artemisinin (1.0 equiv, 0.34 mmol), MB (0.2 equiv), *N*-benzyl-1,4-dihydronicotinamide (BNAH, 4.0 equiv), air, 20 °C, 24 h; 4. as for 3, under argon. [b] Based on reacting artemisinin.

reduced ~26% of the flavin (Figure 3). Next, when LF (0.2 equiv) was treated with BNAH (2.0 equiv) in the presence of artemisinin **1** (1.0 equiv), **1** was reduced to the 2-deoxy products **17** and **25** within 80 min (Table 2). Small amounts of other uncharacterised materials were also formed, as indicated by ¹H NMR spectra recorded on reaction mixtures. However,

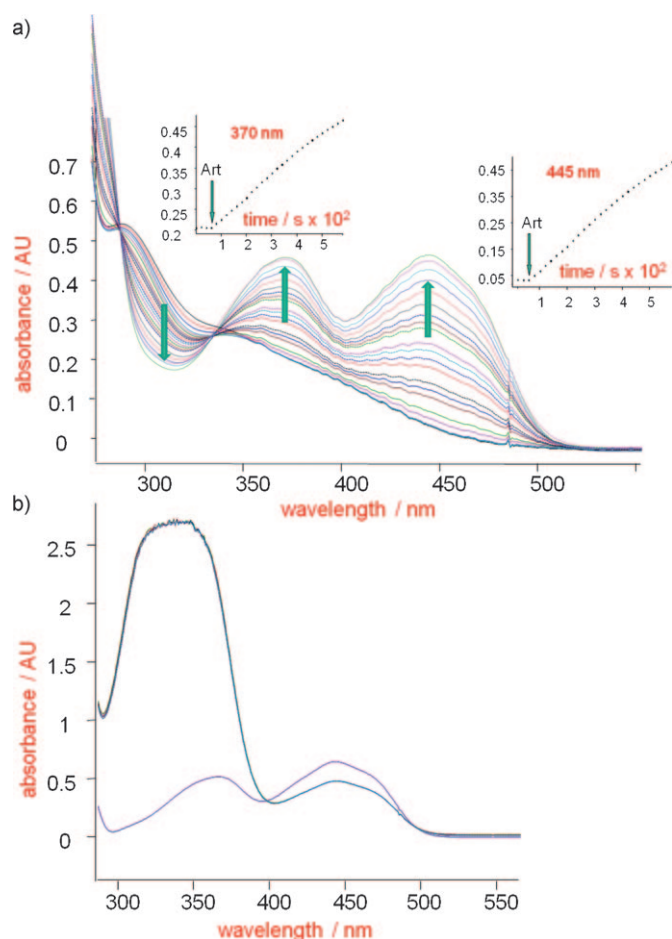


Figure 3. a) Oxidation of reduced riboflavin (RFH₂) **11** by artemisinin **1**: a solution containing 6.6×10^{-4} mmol RF at 37 °C treated with sodium dithionite (1.4×10^{-2} mmol) under argon results in complete reduction of the RF to RFH₂ (disappearance of absorption at λ 370 and 445 nm). This solution is treated with a solution of artemisinin **1** (Art, 4×10^{-4} mmol) in MeCN with monitoring of absorption at λ 370 and 445 nm every 20 s until complete oxidation had taken place (within 10 min). b) Partial reduction of RF by NADH: 1. A buffer solution of RF containing 9.9×10^{-5} mmol RF gives a spectrum with an absorption of 0.67 at λ 445 nm; 2. The solution is treated with a buffer solution containing 9.1×10^{-4} mmol NADH; absorption at λ 445 nm is 0.5. This corresponds to a reduction of ~26% of the RF to RFH₂.

these compounds could not be isolated. Further details are given in the Experimental Section below and in the Supporting Information. DHA **2**, over the course of 80 min, gave deoxy-DHA **19**, 9-epi-2-deoxyDHA **19e**, and the tricarbonyl compound **20**. Notably, the peroxyhemiacetal **26**, which possesses potent antimalarial activity in vitro,^[39] was rapidly converted into the same products. Reactions with RF, although slower, had identical outcomes (Table 2). The course of the reaction was readily followed by withdrawing aliquots from the reaction mixture at 30 min intervals, and examining the NMR spectra. An example of a time-course experiment with artemisinin and the RF–BNAH system is given in the Supporting Information, and is indicative of the cleanliness of these reactions. With flavin mononucleotide (FMN) **12** or FAD **14** (0.2 equiv) and NADH or NADPH (each 2 equiv) in MeCN/pH 7.4 buffer under argon, **1** provided the deoxy products **17** and **25**. The reaction

Table 2. Yields of products from flavin–dihydroflavin redox-mediated decomposition of artemisinins **1–5** and peroxyhemiacetal **26**.

Artemisinin: R (Figure 1) or peroxide	Method ^[a]	Artemisinin remaining and product yields [%] ^[b]
1 : artemisinin R=O	1. LF–BNAH, Ar, 80 min	1 : 0, 17 : 14, 25 : 54
	2. RF–BNAH, Ar, 3 h	1 : 5, 17 : 26, 25 : 48
	3. FMN–BNAH, Ar, 3 h	1 : 4, 17 : 26, 25 : 55
	4. FAD–NADH, Ar, 3 h	1 : 9, 17 : 19, 25 : 49
	5. FAD–NADPH, Ar, 3 h	1 : 17, 17 : 17, 25 : 48
1e : 9-epiartemisinin R=O	2. RF–BNAH, Ar, 3 h	1e : 50, 17e : 5, 25e : 53
2 : DHA R=OH	1. LF–BNAH, Ar, 80 min	2 : 8, 19 : 42, 20 : 19, 19e : 9
	2. RF–BNAH, Ar, 3 h	2 : 0, 19e : 77
3 : artemether R=OCH ₃	1. LF–BNAH, Ar, 2.5 h	3 : 3, 19 : 17, 20 : 18, 19e : 48
	2. RF–BNAH, Ar, 3 h	3 : 0, 19 : 12, 20 : 5, 19e : 52
4 : artesunate	6. FAD–NADPH, Ar, 3 h	4 : 1, 19 : 92, 20 : 5
5 : artemisone	1. LF–BNAH, Ar, 6 h	5 : 0, 19 : 12, 20 : 11, 19e : 42
26 : peroxyhemiacetal	1. LF–BNAH, Ar, 80 min	26 : 0, 19 : 38, 20 : 8, 19e : 5

[a] Reactions performed in 1:1 MeCN/aqueous buffer (pH 7.4), except in 6 below, in which pH 7.4 aqueous buffer alone is used: 1. artemisinin (1.0 equiv, 0.17 mmol), lumiflavine (LF, 0.2 equiv), BNAH (2.0 equiv), argon, 20 °C, 1–6 h; 2. artemisinin (1.0 equiv, 0.17 mmol), riboflavin (RF, 0.2 equiv), BNAH (2.0 equiv), argon, 20 °C, 3 h; 3. artemisinin (1.0 equiv, 0.17 mmol), FMN (0.2 equiv), BNAH (2.0 equiv), argon, 20 °C, 3 h; 4. artemisinin (1.0 equiv, 83.94 μ mol), FAD (0.2 equiv), NADH (2.0 equiv), argon, 20 °C, 3 h; 5. artemisinin (1.0 equiv, 50.65 μ mol), FAD (0.20 equiv), NADPH (2.0 equiv), argon, 20 °C, 3 h; 6. artesunate (1.0 equiv, 33.56 μ mol), FAD (0.2 equiv), NADPH (2.0 equiv), argon, 20 °C, 3 h. [b] Based on reacting artemisinin.

with artesunate **4** does not require MeCN as co-solvent; artesunate is appreciably soluble in pH 7.4 buffer,^[3] and it was efficiently reduced by the FAD–NADPH system within 3 h. With the exception of the artesunate reaction, MeCN was used to assist the solubilisation of the artemisinins. MeCN, used previously as a co-solvent in ferrous iron reactions of artemisinins,^[8–11] does not affect the outcome of the flavin reactions. Tetrahydrofuran, *N,N*-dimethylformamide, and dimethyl sulfoxide (DMSO) may also be used as co-solvents, although with DMSO, the reactions tended to be slower.

9-Epiartemisinin **1e**, with an α -axial methyl group at C9, has significantly lower antimalarial activities than artemisinin **1** in vitro.^[18,40] In direct contrast to **1**, it reacted sluggishly with the BNAH–RF system under the same conditions to return a mixture containing **1e** (50%) and small amounts of the reduction products 2-deoxy-9-epiDHA **17e** and the ring-opened precursor **25e** (Table 2). Under aerobic conditions, all reactions were generally far less effective. For example, artemisinin **1** with RF–BNAH (0.2 and 2 equiv, respectively) after 3 h gave a mixture

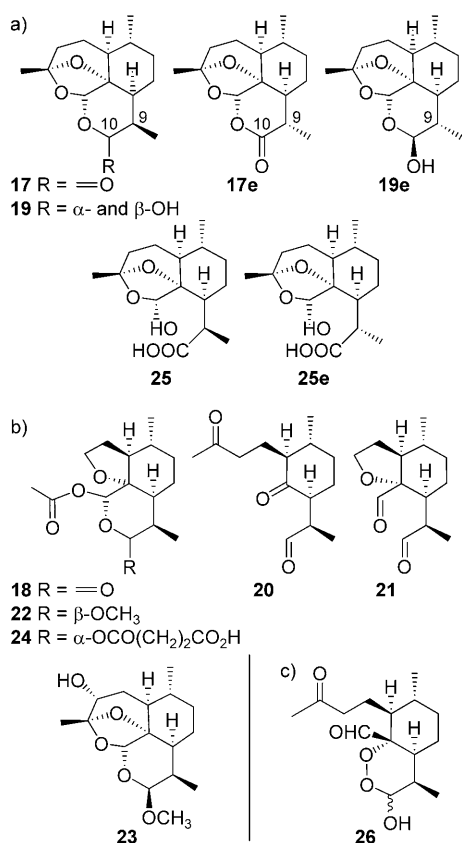


Figure 4. a) Products obtained from artemisinins and catalytic MB–ascorbate, and from MB or flavins and BNAH/NAD(P)H: a) Reduction products. b) Single-electron transfer (SET) products. c) DHA peroxyhemiacetal rearrangement product.

containing unreacted **1** (43%). This may be due to competitive oxidation by oxygen of the dihydroflavin to the flavin,^[27] re-reduction of the flavin eventually exhausts the BNAH.

The artemisinins are more rapidly reduced by the flavin–BNAH or –NAD(P)H systems than by MB–BNAH, even though the same amounts of the reduced conjugates are generated. Treatment of an equimolar mixture of RFH₂ **11** and LMB **7**—generated in aqueous buffer under argon from the precursor mixture and dithionite—with artemisinin **1** resulted in rapid oxidation of RFH₂ (Figure 5). Onset of LMB oxidation took place only when the RFH₂ was oxidised. Significantly, RFH₂ rapidly reduced MB to LMB, confirming the deduction that FADH₂ in parasite GR reduces MB.^[24] In these experiments, it is important to ensure that dithionite does not interfere. This was verified by treating the LMB–RFH₂ mixture with solid NaHSO₄ under argon to destroy excess dithionite,^[10] and adding base to restore the pH to 7.4 prior to treatment with artemisinin.

Effect of artemisinin on NADPH in glutathione reductase

To complement the foregoing, we conducted a preliminary examination of the effects of artemisinin **1** on NADPH consumption during flavoenzyme function. For glutathione reductase (GR), oxidation of FADH₂ by **1** must result in enhanced turnover of NADPH, as the latter reduces FAD back to FADH₂ re-

quired for ultimate conversion of GSSG to reduced glutathione, GSH. As the malaria parasite *P. falciparum* GR (PfGR) was inaccessible, yeast and recombinant human GR were used. Redox behaviour of PfGR resembles that of yeast GR.^[41] Catalytic turnover of MB by PfGR is 100-fold faster than for the human enzyme.^[24] For different GR isoforms, a correlation between NADPH auto-oxidase activity and MB reductase activity is noted. Thus, a comparison of the effect of **1** on yeast and human GR by examination of NADPH turnover is valid. As in other studies,^[24] we ensure that substrate GSSG and cofactor be kept at a fixed ratio and modest excess with respect to the enzyme in order to evaluate the effect of **1** on NADPH turnover. Whilst ideally, we should seek to demonstrate an effect corresponding to the low nanomolar concentrations of artemisinins that normally suffice to exert a parasitocidal effect, in this case, we are dealing with isolated yeast enzyme. Further, it must be borne in mind that artemisinins selectively and irreversibly partition into parasitised erythrocytes.^[42] There is no information on how artemisinins may sequester inside the parasite cytosol to provide the relative concentrations of artemisinins required to subvert the parasite enzyme. Therefore, the important issue here in the first instance is to establish if there is indeed an effect exerted by artemisinins on redox-active flavoenzymes. Treatment of yeast GR with GSSG and NADPH in aqueous buffer at pH 7.4 under argon resulted in consumption of the NADPH. Next, addition of artemisinin **1** (0.5 equiv with respect to NADPH) at the outset *greatly increased* the rate of consumption and decreased the production of GSH (Figure 6 and figure S2, Supporting Information). When the experiment was repeated under aerobic conditions, the consumption of NADPH in the presence of **1** *was further increased*. Moreover, it is shown that at the same concentrations in parallel experiments, artemisinin interferes with production of GSH from GSSG (figure S2, Supporting Information). Control experiments with yeast GR conducted in the presence of GSSG but in the absence of artemisinin indicated that NADPH turnover is no different under argon or under aerobic conditions (figure S3, Supporting Information). Next, a comparison of the effect of **1** on equivalent concentrations of each of yeast and recombinant human GR was carried out. Remarkably, with human GR, there was *no significant change* in turnover of NADPH upon treatment with **1** under either anaerobic or aerobic conditions (Figure 6). Further data from sets of parallel experiments are given in the Supporting Information (figures S4 and S5). Importantly, treatment of artemisinin with reduced glutathione, the product of GR function, in MeCN/pH 7.4 aqueous buffer under argon for 24 h does not induce detectable decomposition of **1**.

Discussion

Chemistry and structure–activity relationships

DHA **2** provides the peroxyhemiacetal **26** (Figure 4) via an open hydroperoxide.^[36] Importantly, its formation under such mild conditions here indicates it must form *in vivo* when DHA **2** or its prodrug artesunate **4** are used as antimalarial drugs. As DHA does not rearrange in the absence of BNAH in aqueous

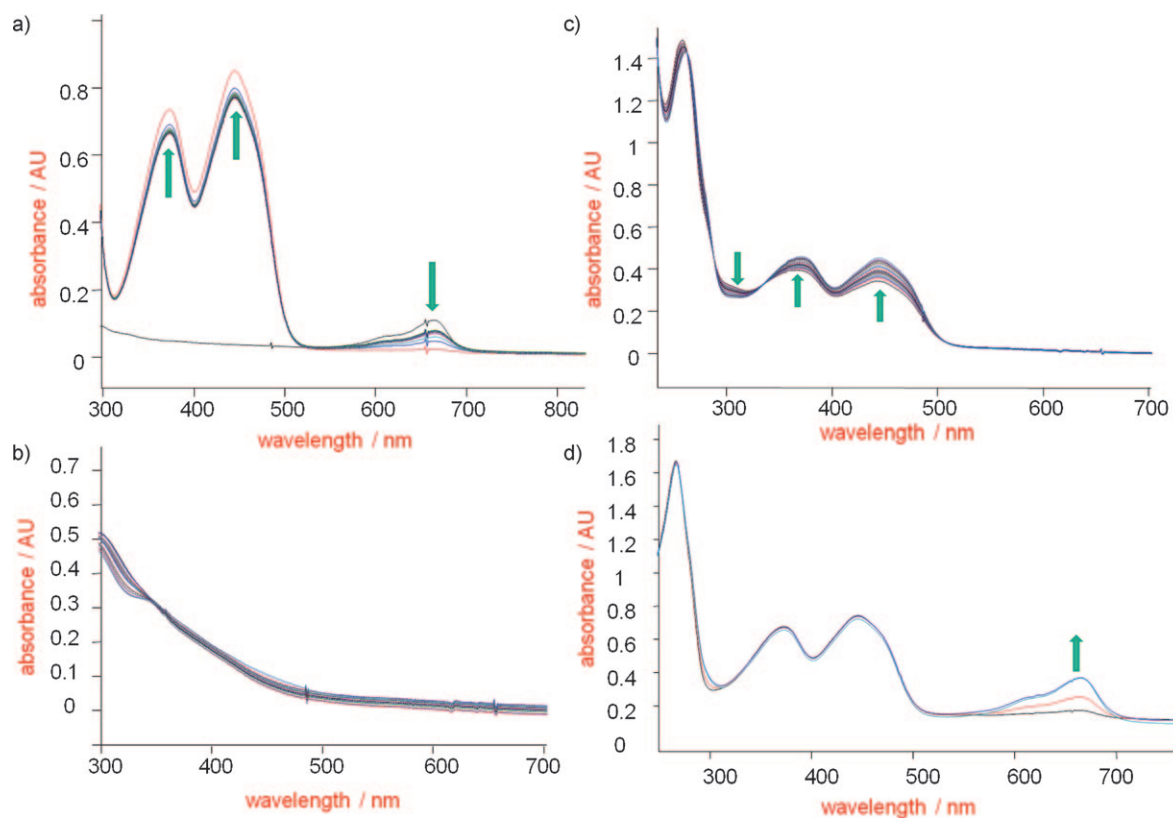


Figure 5. a) Reduction of methylene blue (MB) **6** by excess reduced riboflavin RFH₂ **11**: effect of adding RFH₂ (9×10^{-5} mmol) to MB (9.4×10^{-7} mmol) in aqueous pH 7.4 buffer; absorptions at λ 370 and 445 nm increase due to formation of RF, and the absorption at λ 654 nm from MB decreases to baseline level due to reduction of MB to LMB **7**. b)–d) Oxidation of a mixture of reduced riboflavin RFH₂ **11** and LMB **7** by artemisinin **1**: b) Absorption spectrum of mixture recorded upon complete reduction of RF (9.9×10^{-5} mmol) and MB (9.4×10^{-5} mmol) by sodium dithionite (1.4×10^{-2} mmol) in degassed aqueous buffer at pH 7.4: disappearance of absorptions at λ 450 and 370 nm (flavin), and at λ 654 nm (MB) ($t = 200$ s). c) Effect of adding 2×10^{-3} mmol artemisinin (**1**) in MeCN and monitoring appearance of absorptions at λ 370, 445, and 654 nm: spectra taken between 10–200 s after addition of artemisinin indicate increase of absorptions at λ 370 and 445 nm due to formation of RF. d) Spectra taken between 200–400 s after addition of artemisinin indicate the formation of MB (λ_{max} 650 nm).

buffer, it is apparent that BNAH, as a potent hydrogen bond acceptor, must act to facilitate the proton transfers required for the rearrangement; this is likely initiated via transfer of the proton from the C10 hydroxy group. The unusual C9 epimer of deoxyDHA, namely compound **19e**, likely arises via ring opening of deoxyDHA to the C10 aldehyde that undergoes epimerisation at C9 followed by closure; a related process is known.^[36] Given the mild, biomimetic conditions attending its formation, it is predicted here that compound **19e** should appear among the various metabolites isolated from patients treated with DHA, artemether, or artesunate.

The SET products, at the same oxidation level as the starting artemisinin, are formed with the Fe^{II}–Fe^{III} couple,^[8,9,11] or here from MB, likely via the initiating electron donor, the LMB radical **7**. The electron acceptor is MB, dehydroascorbate (DA), or the ascorbyl radical, and under aerobic conditions, oxygen, leading to superoxide and hydroperoxide (Scheme 1). It is important to note that the pathway leading to the dominant products of the SET process, namely the furano acetates **18**, **22**, and **24**, and the corresponding hydrolysis product **21** from **22** and **24**, is fundamentally different from the energetically demanding insertion of a primary C4 radical into the Fe^{III}–O

bond proposed for the formation of related products in the iron reactions.^[9,11] However, the current reactions are iron free, and the insertion as depicted in Scheme 1 must be favoured kinetically and also have a thermodynamically plausible outcome in providing the relatively stable ketyl radical. The last will itself participate in SET by reducing dehydroascorbate to the ascorbyl radical and oxygen to superoxide. The participation of ketyl radicals in enzyme-mediated pathways, including their oxidation by oxygen, is well established.^[43] The results described herein indicate that the in vivo formation of a furanoacetate related to those described here does not necessarily depend on ferrous iron,^[44] but more likely requires the presence of a natural redox system, such as AA–dehydroascorbate itself, that functions via SET pathways in the presence of an incipient electron donor or acceptor.

For the MB–BNAH, flavin–BNAH, and flavin–NAD(P)H systems, hydride transfer from LMB or dihydroflavin generated in situ results in reductive cleavage of the peroxide in artemisinin and oxidation of LMB to MB or dihydroflavin to flavin (Scheme 2). MB or flavin, in turn, is reconverted by excess BNAH or NAD(P)H into the reduced conjugates in a catalytic cycle that continues until the artemisinin is consumed. For the

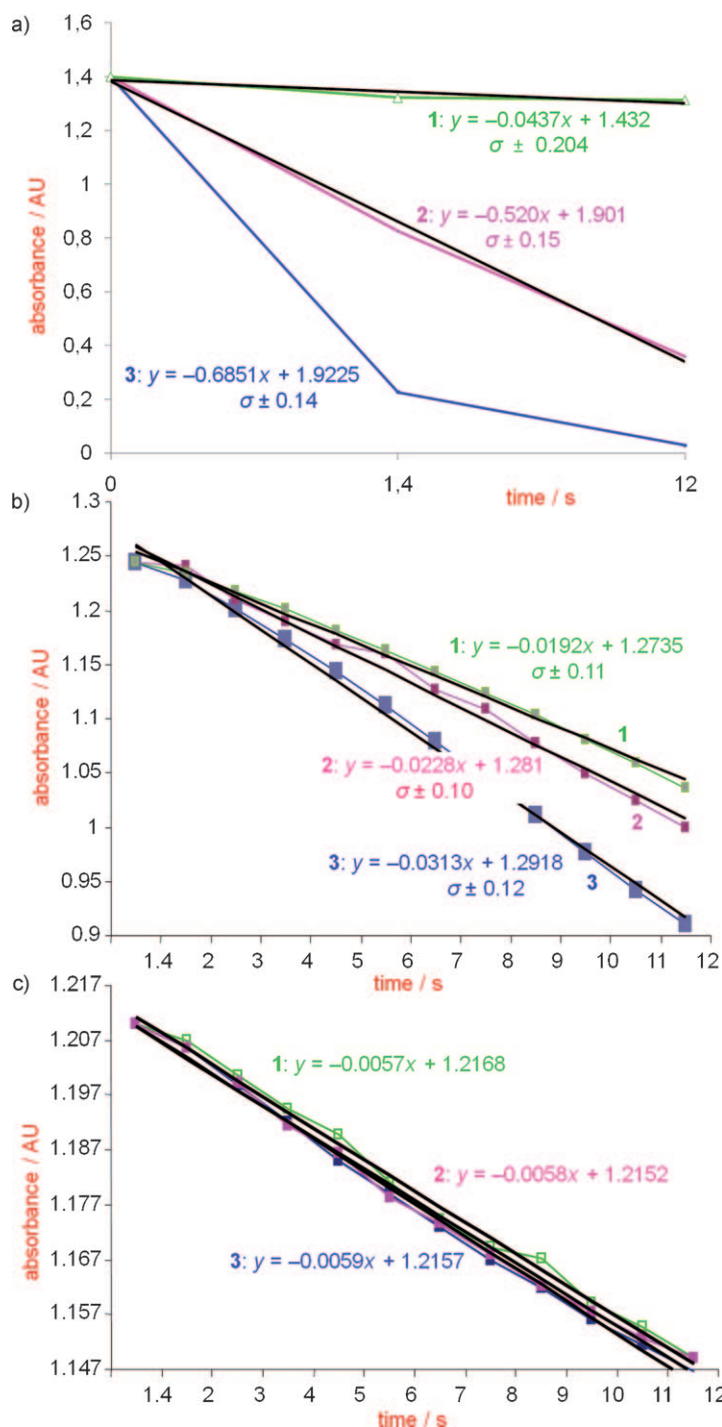
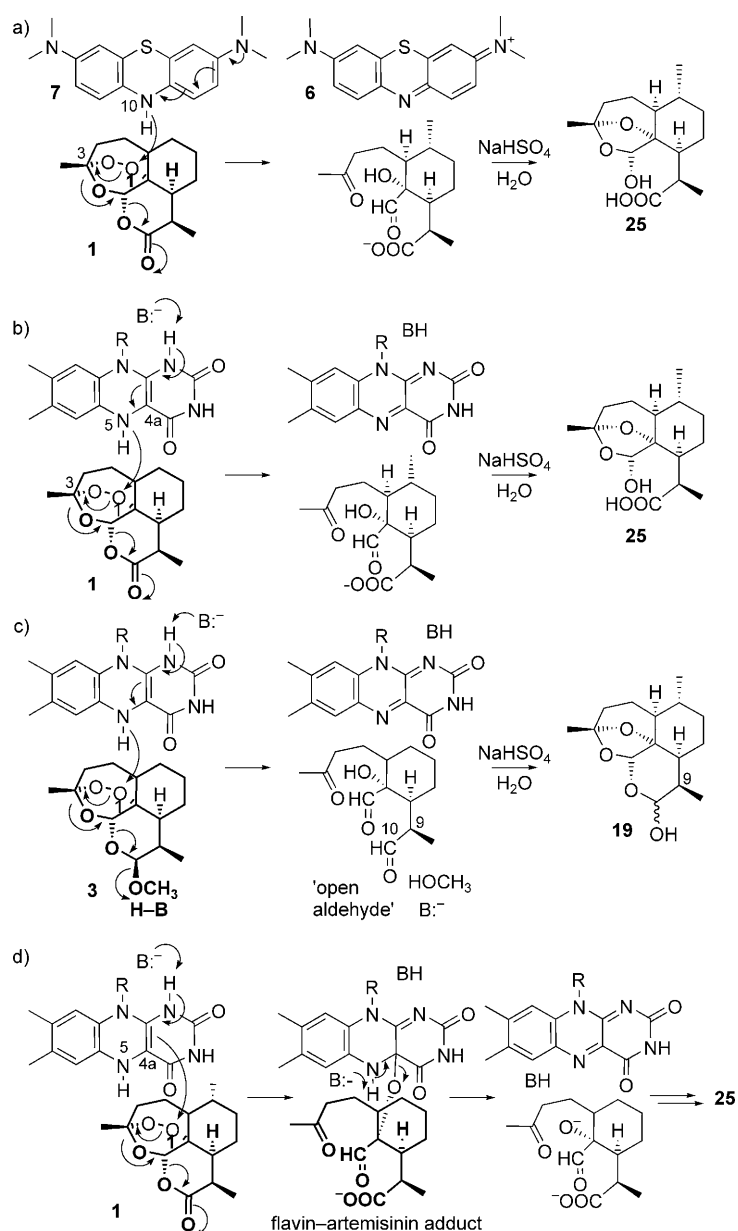


Figure 6. a) Effect of artemisinin 1 on NADPH turnover in yeast GR, and comparison between yeast and human GRs at equal enzyme concentrations; rate of NADPH turnover monitored at λ 340 nm for 12 s. a) 1. (green) in MeCN/buffer (pH 7.4); GSSG (4.8×10^{-4} mmol), NADPH (4.8×10^{-4} mmol), GR (1.65 EU) under argon; 2. (maroon), as for 1 + artemisinin 1 (2.4×10^{-4} mmol 1); 3. (blue) as for 2 under air. b) in MeCN/buffer (pH 7.4); NADPH (4.8×10^{-4} mmol), GSSG (4.8×10^{-4} mmol), yeast GR (0.33 EU). 1. (green), control (GSSG, NADPH, GR); 2. (maroon) effect of 1 (2.4×10^{-4} mmol 1); 3. (blue) repetition of 2 under air. c) As for part b), but with pH 6.8 buffer with recombinant human GR (0.35 EU), and NADPH–GSSG as in b). 1. (green) control; 2. (maroon) effect of addition of artemisinin 1; 3. (blue) repetition of 2 under air. Details of other experiments including controls and additional figures S2–S6 are given in the Supporting Information.

dihydroflavins, a close analogy is provided by hydride-induced cleavage of cysteine disulfide mediated by FADH_2 within disulfide reductases during the catalytic cycle preceding generation of GSH from GSSG.^[25] Indeed, it was the knowledge of this pathway that suggested to us that the cleavage of the peroxide in artemisinin via hydride transfer from dihydroflavins should occur. Another example is provided by hydride reduction of quinones mediated by FADH_2 in NAD(P)H–quinone oxidoreductases (diaphorases).^[45] According to Scheme 2, it is important to note that as the peroxide is embedded in a trioxane core that is coupled inductively to more remote oxygen atoms, hydride transfer will drive ring opening of artemisinin 1 to provide the open deoxyartemisinin precursor 25. For each of the artemisinins 2–5, hydride transfer leads to loss of hydroxy, methoxy, succinyl, and thiomorpholine-*S,S*-dioxide residues, respectively, to give the open aldehyde that closes to 19, or via prior epimerisation at C9, to 19e. At pH 7.4, each of ionised LMB 7^- ($\text{p}K_a$ LMB ~ 5)^[24] and dihydroflavin ($\text{p}K_a$ LFH₂ ~ 6)^[27] are present, and adduct formation (Scheme 2) is feasible. This is accommodated by the potent nucleophilicities of the negatively charged nitrogen activated by the *para-N,N*-dimethylamino group in 7^- , and of the deprotonated enamine (enamide) in the dihydroflavin, wherein adduct formation with electrophiles is reported to be particularly facile.^[46] Nevertheless, examination of product mixtures obtained after neutral workup of the reaction of 1 with the LF–BNAH system under argon has not yet provided evidence for flavin–artemisinin adducts. However, at least in the case of yeast GR *in vitro* under the conditions described herein, it is unlikely that such adducts can be stable, or metastable, as the accelerated turnover of NADPH in yeast GR in the presence of the artemisinin implies that turnover of the flavin cofactor is also increased. However, this issue may become more important in an *in vivo* situation with flavoenzymes, for if the artemisinin–flavin adducts are stable, or metastable, this may imply irreversible blockade, or suppressed turnover, of the cofactor, as discussed below.

The reduction of the artemisinins by dihydroflavins correlates with structure–activity profiles of artemisinins and analogues for which an α -axial methyl group at C9^[18,40] or bulky α groups in the hydrocarbon periphery^[47] that buttress the peroxide suppress antimalarial activities. Such groups must act to restrict or actually inhibit the approach by dihydroflavin to the peroxide required for hydride transfer to, or adduct formation at, O1 (Scheme 2). This is borne out by the sluggish reactivity of 9-epiartemisinin 1e (Table 2). The electronically coupled processes shown in Scheme 2 rely on transmission of inductive effects via the non-peroxidic oxygen atom of the trioxane core to the more remote oxygen atoms that renders O1, *but not* O2, susceptible to addition of hydride (or of the dihydroflavin, if adduct formation occurs). Examples of the manner in which such inductive effects modulate the properties of artemisinins have been described previously.^[48] The importance of the trioxane in modulating antimalarial properties is incisively demonstrated in elegant synthetic studies wherein replacement of the non-peroxidic oxygen atom of the trioxane core by a methylene group suppresses antimalarial activities to 3–24% of those of the corresponding artemisinin, even though



Scheme 2. Reduction of artemisinin **1** and artemether **3** by LMB **7** or reduced flavins. Generation of LMB **7** from MB **6** or dihydroflavin from the flavin in situ is coupled with oxidation of BNAH to BNA⁺ or of NAD(P)H to NAD(P)⁺. Oxidation of the reduced conjugates by the artemisinin regenerates MB or flavin, which in turn is reduced in a catalytic cycle by the excess of BNAH or NAD(P)H (not shown). a) Leucomethylene blue **7** or b) dihydroflavin transfers hydride to O1 of artemisinin **1** to generate MB or flavin and **25**. c) Hydride transfer to artemether **3** drives ring opening with loss of methoxyl. d) Adduct formation from reaction of dihydroflavin enamide through **4a** with O1 of artemisinin **1** and collapse of adduct to generate flavin. Equivalent processes may involve prior deprotonation at, and reaction through, N5 of the dihydroflavin or through N10 of 7⁻ (BH and B⁻ proton source and base in the reaction medium; the C5a H atom and C6 methyl group of artemisinins in some intermediate structures are omitted for clarity).

the parent artemisinins and derived structures are superimposable.^[49] In other words, 1,2,4-trioxanes are intrinsically more active as antimalarial drugs than their 1,2-dioxane counterparts.^[50] Finally, we note that the 5-*nor*-4,5-*seco*-artemisinin analogue **27** (Figure 1) made by total synthesis possesses an *in vitro* antimalarial activity roughly equivalent with that of arte-

misinin.^[51] Such a compound is distinctly less capable of forming C radicals once the peroxide bridge undergoes cleavage by Fe^{II} in the Fenton reaction,^[52] but the *intact* peroxide within the trioxane is clearly capable of accepting hydride from FADH₂.

Flavoenzyme target and ramifications for anti-malarial activities of artemisinins

It has been reported previously that a lack of FAD may confer substantial protection from severe malaria.^[23] In addition to PfGR, other flavoenzymes that show enhanced turnover of MB (initiated via reduction of the MB by the reduced flavin), for example TrxR or dihydroipoamide dehydrogenase,^[23] are possible targets for artemisinins. It is suggested that the ability of the intra-erythrocytic parasite to hold oxidative stress in check through an intense glutathione metabolism thereby must be disrupted by artemisinin. The even greater turnover of NADPH exerted by artemisinin under aerobic conditions indicate that autoxidation of FADH₂ by oxygen takes place.^[27,28] This correlates with the ability of artemisinins to generate ROS^[14,17] and indicates that incipient oxidation of FADH₂ by artemisinins interferes either with the amino acid gate that inhibits ingress of oxygen^[53] or with the intimate stacking arrangement required for hydride transfer from NADPH to FAD. Thereby FADH₂ becomes accessible to oxygen.^[24,25,28] The synergism between MB and artemisinins arises as both drugs enhance turnover of NADPH by each oxidising FADH₂. Artemisinins also re-oxidise LMB, thus accelerating the futile cycling of NADPH with MB. Enhanced turnover of MB and of ROS is also apparent in the SET processes involving artemisinins and MB under aerobic conditions (Scheme 1).

The implication of flavoenzymes as targets for artemisinins brings into focus a large body of data relating to the effect of inhibitors on flavoenzymes at large. Thus, in another sense, if the residue arising via reduction of the artemisinin by the dihydroflavin *in vivo* remains noncovalently linked (by hydrogen bonding,^[54] for example) to the flavin such as FAD, and needs to diffuse away to expose the flavin to reduction by NADPH, then at the least, GR or TrxR function, for example, will be slowed. Although the role of antimalarial redox-active substrates MB, and antimalarial flavins and riboflavin, in generating ROS is discussed above,^[25,26] an additional consideration is that such substrates including redox-active quinones and their hydroquinone conjugates^[55] may form π complexes or hydrogen bonded noncovalent adducts with the FAD, and thus interfere, both physically and through modulation of redox potential,^[56] with transfer of reducing equivalents from NADPH.

The greater sensitivity to artemisinins of yeast GR, used here as a surrogate for parasite GR, in comparison with the relative

lack of sensitivity of human GR provides a putative model to explain the pronounced cytotoxicities of artemisinins against the malaria parasite vis-à-vis mammalian cell lines. However, those factors^[24] that render yeast (or parasite) GR more susceptible than human GR to each of MB and the artemisinins must be clarified. The putative difference in sensitivities between parasite and human GR to artemisinins further suggests the malaria parasite either may acquire resistance through mutations that render the parasite flavoenzyme structurally more akin to the human enzyme, or it may enhance the use of intrerythrocytic GR, that is unaffected by artemisinins, for maintenance of redox balance.^[25,57,58] A point of focus in this regard may be the binding of NADPH in the parasite GR active site that differs from the human enzyme. Replacement of His219 in the human enzyme by Gly207 in the parasite enzyme makes for a less tenacious binding of NADPH,^[25] and this may have an effect on the parasite GR system when under assault by artemisinins.

Conclusions

In summary, artemisinins act both as one-electron transfer agents and two-electron acceptors in the absence of iron. They are likely to interfere with flavin cofactors of redox-active intraparasitic enzymes. Given that structurally simpler antimalarial-active peroxides^[59] likely interact with the same systems, the design of new artemisinins and analogues may therefore more fruitfully refocus on a consideration of activity against flavoenzymes. The susceptibility of flavin cofactors has ramifications well beyond malaria chemotherapy, as artemisinins are active against other parasitic and non-parasitic pathogens.^[16,60] In particular, the behaviour of artemisinins disclosed herein directs attention to the possibility of artemisinins interfering with diaphorases and other flavoenzymes important in tumorigenesis, where now, among others, the flavin cofactors in redox-active thioredoxin reductase (TrxR)^[61] and DT-diaphorase^[62] must be considered as potential targets.

X-ray crystal structure determination of 9-epideoxyDHA 19e

A crystal specimen of dimensions 0.30×0.14×0.12 mm³ was used for collection of a full sphere of diffraction data to $\theta = 67.5^\circ$ on an Oxford Diffraction Gemini CCD diffractometer at 173 K using copper (CuK α) radiation. The crystal belongs to the monoclinic system with chiral space group *P*2(1). The molecular structure was successfully solved and refined to $R_1 = 0.0280$, $wR_2 = 0.0743$ and indicates the molecule to be 9-epideoxydihydroartemisinin, C₁₅H₂₄O₄, compound **19e**. A summary of crystallographic data is listed in Table 3, and the data have been deposited with the Cambridge Crystallographic Data Centre: CCDC 782559 (**19e**) contains the supplementary crystallographic data for this paper. These data can be obtained free of charge from The Cambridge Crystallographic Data Centre via www.ccdc.cam.ac.uk/data_request/cif.

The absolute configuration of the compound is supported by refinement of the Flack parameter to a value of $-0.04(8)$ and indicates the configuration of 9S,10S for the stereochemi-

Table 3. Crystallographic data for compound **19e**.

Parameter	Value
empirical formula	C ₁₅ H ₂₄ O ₄
formula weight [Da]	268.34
temperature [K]	173(2)
wavelength [Å]	1.54178
crystal system	monoclinic
space group	<i>P</i> 2(1)
unit cell dimensions [Å]	$a = 13.73020(10)$, $\alpha = 90^\circ$ $b = 9.12650(10)$, $\beta = 96.1610(10)^\circ$ $c = 17.1569(2)$, $\gamma = 90^\circ$
volume [Å ³]	2137.49(4)
Z	6
density (calcd) [mg m ⁻³]	1.251
absorption coefficient [mm ⁻¹]	0.724
<i>F</i> (000)	876
crystal size [mm]	0.30×0.14×0.12
θ range for data collection	2.59–67.47°
index ranges	$-16 \leq h \leq 16$, $-9 \leq k \leq 10$, $-20 \leq l \leq 20$
reflections collected	30038
independent reflections	7238 [$R(\text{int}) = 0.0254$]
completeness to $\theta = 66.50^\circ$	99.4%
absorption correction	semiempirical from equivalents
maximum transmission	1.00
minimum transmission	0.59
refinement method	full-matrix least-squares on F^2
data/restraints/parameters	7238/1/514
goodness-of-fit on F^2	1.019
final <i>R</i> indices [$I > 2\sigma(I)$]	$R_1 = 0.0280$, $wR_2 = 0.0734$
<i>R</i> indices (all data)	$R_1 = 0.0294$, $wR_2 = 0.0743$
absolute structure parameter	$-0.04(8)$
largest diff. peak and hole [e Å ⁻³]	0.158 and -0.135

cal centers of interest. The molecular geometry for all three crystallographically independent molecules is very similar, in each case with a twist-boat conformation found for the pyran ring containing the hemiacetal functionality. Typical displacements from the mean plane for the ring atoms are C₁ 0.00, C₁₂ -0.32 , C_{8a} $+0.31$, C₉ 0.00, C₁₀ -0.35 , and O₁₁ $+0.37$ Å. This rather unusual arrangement is to decrease axial interactions between the C₉ methyl substituent and O₁, the residual pyran oxygen remaining from the peroxide functionality of the

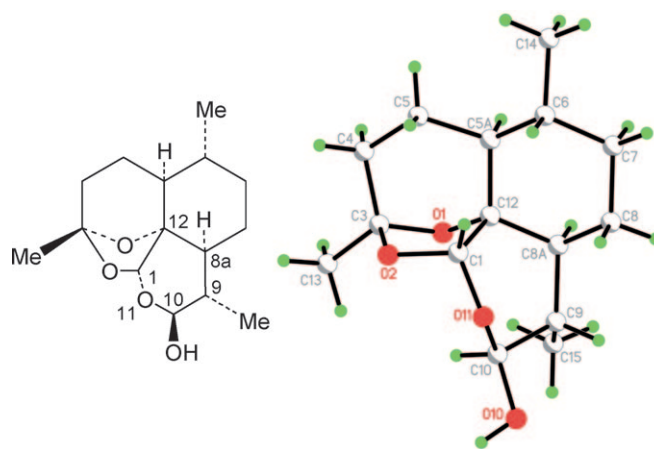


Figure 7. Labelling scheme for compound **19e** (at left). Structure of **19e** showing one of the three crystallographically independent molecules (right).

parent compound, which are unfavorable for a chair configuration, as confirmed by MM2 molecular dynamics simulation. The labelling scheme for compound **19e** and structure showing one of the three crystallographically independent molecules is shown in Figure 7.

Experimental Section

Artemisinins **1–3** were supplied by the Kunming Pharmaceutical Corporation (China), artesunate **4** was supplied by Dr. Robert Carter, Abbott–Knoll AG, Basel (Switzerland), and each of artemisone **5**^[3] and 9-epiartemisinin **1e**^[40] were prepared according to published procedures. Methylene blue (certified, BSC, Sigma–Aldrich), L-(+)-ascorbic acid (>99%, puriss, Sigma–Aldrich), nicotinamide (Aldrich, ≥99%), lumiflavine (>97%, Sigma), riboflavin (98%, Acros), FMN (73–79%, Sigma), FAD (≥95%, Sigma), NADH (97%, Sigma), NADPH (~90%, Fluka), reduced L-glutathione (≥98%, Sigma–Aldrich), glutathione reductase from baker's yeast, ammonium sulfate suspension, 100–300 U(mg protein⁻¹; Sigma) and human glutathione buffered aqueous solution, ≥12 U(mg protein⁻¹, recombinant; Sigma) were used as received. All reactions were carried out under an atmosphere of air or argon as indicated. The solvents ethyl acetate and hexane were distilled prior to use: ethyl acetate from magnesium sulfate and hexane from calcium chloride. Column chromatography was performed with Merck silica gel 60 (0.04–0.063 mm). UV/Vis spectra were recorded on an Agilent 8453 instrument, and ¹H and ¹³C NMR spectra were obtained as solutions in CDCl₃ on a Bruker AV 400 spectrometer operating at 400 and 100 MHz, respectively. CDCl₃ was used as solvent unless otherwise stated. Melting points were carried out on an Leica Hot Stage DME E compound Microscope and are corrected. Mass spectral data were obtained on an API QSTAR high-performance triple quadrupole time-of-flight mass spectrometer with electrospray ionisation, and on a Waters Micromass GCT premier ToF high-resolution mass spectrometer (CI+, methane). Infrared spectra were recorded on a Perkin–Elmer PC 16 spectrometer. Single-crystal X-ray structure measurements were carried out on a Bruker Smart-APEX CCD four-circle diffractometer or an Oxford Xcalibur PD X-ray diffractometer Cu source.

N-Benzyl-1,4-dihydronicotinamide 16: This was prepared by the following modification of the published procedure.^[63] A stirred solution of nicotinamide (5 g, 0.041 mol) and benzyl bromide (6.33 mL, 0.053 mol, 1.3 equiv) in THF (50 mL) under nitrogen was heated under reflux at an oil bath temperature of 80 °C for 6 h. After 6 h, the mixture was concentrated under reduced pressure. The residual solid was washed with hexane into a sintered glass funnel, and the white solid so obtained was dried under high vacuum. The *N*-benzylnicotinamide (9.36 g, 78%) was used without further purification: ¹H NMR ([D₆]DMSO): δ = 5.94 (s, 2H), 7.41–7.43 (m, 3H), 7.57–7.60 (m, 2H), 8.19 (s, 1H), 8.25–8.30 (t, 1H), 8.63 (s, 1H), 8.97–8.99 (d, 1H, *J* = 8.2 Hz), 9.33–9.35 (d, 1H, *J* = 5.8 Hz), 9.68 ppm (s, 1H). A mixture of the *N*-benzylnicotinamide (3.87 g, 13.2 mmol) was stirred with sodium carbonate (7.14 g, 67.4 mmol, 5.1 equiv) in deionised water (93 mL) at 20 °C under nitrogen resulting in the formation of an orange-coloured solution. Sodium dithionite (9.19 g, 52.8 mmol, 4.0 equiv) was added slowly. The reaction mixture was stirred for 4 h, during which time the mixture became yellow with eventual formation of a yellow precipitate. The precipitate was collected by filtration, thoroughly washed with water, and dried under reduced pressure to obtain a yellow solid (2.60 g, 92%) that was dried under high vacuum, and then stored in the dark under argon. The *N*-benzyl-1,4-dihydronicotinamide **16**

was able to be recrystallised from dichloromethane to give pale-yellow plates, mp: 118.5–119.5 °C; ¹H NMR: δ = 3.16 (d, 2H, *J* = 1.5 Hz), 4.28 (s, 2H, -CH₂Ph), 4.72–4.77 (m, 1H), 5.39 (s, 2H, NH₂), 5.73 (dd, 1H, *J* = 1.4, 1.4 Hz), 7.15 (d, 1H, *J* = 0.8 Hz), 7.22–7.38 ppm (m, 5H, ArH); MS (CI) C₁₃H₁₄N₂O calcd for [M+1] 215.1184, found: 215.1182. However, the material prior to recrystallisation was of sufficient purity for use in the catalytic experiments; purity before use was checked by ¹H NMR spectroscopy.

UV/Vis absorption spectroscopy

1. Leucomethylene blue (LMB)–artemisinin (Figure 2a and figure S1, Supporting Information): MB (5 mg, 0.015 mmol) in phosphate buffer (pH 7.4, 5 mL) under argon was treated with sodium dithionite (10 mg, 0.14 mmol) resulting in the disappearance of absorption at λ 654 nm, and a colour change from blue to pale-yellow as **7** was formed. This solution (1 mL), containing **7** (3.1 × 10⁻³ mmol) in MeCN/aqueous pH 7.4 buffer (1 mL) under argon was injected into a UV cuvette. Next, a solution of artemisinin **1** (1.7 × 10⁻³ mmol in 0.1 mL MeCN) was injected into the UV cuvette containing the solution of **7**. The resulting solution was stirred continuously whilst spectra were recorded at ~1 min intervals from 0–10 min, when no further oxidation of **7** took place. Repetition of the reduction of MB by dithionite and extracting the LMB into dichloromethane followed by a UV/Vis study of the effect of artemisinin on LMB in the dichloromethane solution is described in the Supporting Information.

2. Reduction of methylene blue (MB) by NADH (Figure 2b): A solution was prepared from MB **6** (2.0 mg) and degassed pH 7.4 aqueous buffer (1 mL) to give a final concentration of 6 × 10⁻³ mmol mL⁻¹. This solution (100 μL) was diluted by the addition of degassed buffer (4 mL) to generate a solution containing 1.5 × 10⁻⁴ mmol mL⁻¹; 0.5 mL of the solution, containing 7.8 × 10⁻⁵ mmol MB was placed in the cuvette at 37 °C. The cuvette was sealed with a septum and argon was circulated through the cuvette whilst the solution was magnetically stirred. The spectrum was recorded; *A* = 1.62 at λ 663 nm (spectrum 1). Next, the NADH solution was prepared from NADH (3.0 mg) and degassed pH 7.4 aqueous buffer (3 mL) to give a final concentration of 1.4 × 10⁻³ mmol mL⁻¹ NADH; 1.0 mL of this solution, containing 1.5 × 10⁻³ mmol NADH was injected into the cuvette. *A*_{max} = 1.18 at 663 nm (spectrum 2), corresponding to a reduction of ~28% of the MB to LMB.

3. Oxidation of reduced riboflavin (RFH₂) **11 by artemisinin **1** (Figure 3a):** Riboflavin (RF) **10** (5 mg) was dissolved in degassed 1:1 MeCN/pH 7.4 buffer (2 mL) and 100 μL of this solution was diluted by addition of degassed water (900 μL) to generate a solution containing 6.6 × 10⁻⁴ mmol RF in the UV cuvette at 37 °C. Solid sodium dithionite (1 mg, 1.4 × 10⁻² mmol) was then added. The cuvette was sealed with a septum, and argon was circulated through the cuvette whilst the solution was magnetically stirred. Once complete reduction of the RF had taken place, as gauged by disappearance of absorptions at λ 445 and 370 nm, a solution of artemisinin **1** in MeCN (40 μL containing 4 × 10⁻⁴ mmol **1**) was injected into the cuvette. Absorptions at λ 370 and 445 nm were monitored every 20 s until complete oxidation had taken place (within 10 min).

4. Reduction of riboflavin (RF) by NADH (Figure 3b): RF **10** (3 mg) was dissolved in degassed pH 7.4 buffer (2 mL), and 100 μL of this solution was diluted by addition of degassed buffer (4 mL) to generate a solution containing 9.9 × 10⁻⁵ mmol mL⁻¹ RF; 1 mL (9.9 × 10⁻⁵ mmol) of the solution was placed in the cuvette at

37 °C. The cuvette was sealed with a septum, and argon was circulated through the cuvette whilst the solution was magnetically stirred. The spectrum 1 was recorded, with $A=0.67$ at λ 445 nm. The NADH solution was prepared from NADH (3.0 mg) and degassed pH 7.4 aqueous buffer (3 mL) to give a final concentration of 1.4×10^{-3} mmol mL⁻¹. The solution (650 μ L) containing 9.1×10^{-4} mmol NADH was injected into the cuvette. The spectrum 2 was recorded, with $A=0.5$ at λ 445 nm. This corresponds to a reduction of ~26% of the RF to RFH₂.

5. Reduction of methylene blue (MB) 6 by excess reduced riboflavin RFH₂ 11 (Figure 5a): Methylene blue (2.4 mg) was dissolved in pH 7.4 buffer (2 mL), and 10 μ L of this solution was diluted by addition of buffer (3.99 mL) to generate a solution containing 9.4×10^{-6} mmol mL⁻¹ MB; 0.1 mL of this solution containing 9.4×10^{-7} mmol MB was placed in the cuvette at 37 °C and diluted with 0.9 mL degassed buffer. The cuvette was sealed with a septum, and argon was circulated through the cuvette whilst the solution was magnetically stirred. RF (3 mg) was dissolved in pH 7.4 phosphate buffer (2 mL), and 100 μ L of this solution was diluted by the addition of phosphate buffer (3.99 mL) to generate a solution containing 9×10^{-5} mmol mL⁻¹; 1 mL of this solution containing RF (9×10^{-5} mmol) was injected into a cuvette under argon, and then solid sodium dithionite (1 mg, 1.4×10^{-2} mmol) was added. Argon was circulated through the cuvette whilst the solution was magnetically stirred. After reduction, excess dithionite was removed by careful treatment with solid NaHSO₄. The elimination of dithionite was monitored by disappearance of the absorption from dithionite at λ 320 nm. Solid Na₃PO₄ was then added to restore the solution to pH 7.4. The solution (under argon) was transferred to the first cuvette. Absorptions at λ 370, 445, and 654 nm were monitored every 5 s (within 200 s) (Figure 5a); however, due to the time scale of the experiment, it was not possible to monitor incipient reduction of MB or of oxidation of the reduced riboflavin immediately after mixing.

6. Oxidation of reduced riboflavin RFH₂ 11 and leucomethylene blue LMB 7 by artemisinin 1 (Figure 5b–d): RF 10 (3 mg) was dissolved in degassed pH 7.4 buffer (2 mL), and 100 μ L of this solution was diluted by the addition of degassed buffer (4 mL) to generate a solution containing 9.9×10^{-5} mmol mL⁻¹ RF; 1 mL (9.9×10^{-5} mmol) of the solution was placed in the cuvette at 37 °C. A solution of MB in degassed pH 7.4 buffer (1 mL containing 9.4×10^{-5} mmol) was added. Solid sodium dithionite (1 mg, 1.4×10^{-2} mmol) was then added. The cuvette was sealed with a septum, and argon was circulated through the cuvette whilst the solution was magnetically stirred. The absorption spectra are given in Figure 5b: absorption spectrum of mixture recorded upon complete reduction of RF and MB; the disappearance of absorptions at λ 370 and 450 nm (flavin), and at λ 650 nm (MB) ($t=200$ s) are apparent. A solution of artemisinin (60 μ L, containing 2×10^{-3} mmol artemisinin 1) was injected into the cuvette and appearance of absorptions at λ 370, 445, and 650 nm were monitored every 10 s. Spectra taken between 10–200 s after addition of artemisinin indicate increase of absorptions at λ 370 and 445 nm due to formation of flavin (Figure 5c). Spectra taken between 200–400 s after the addition of artemisinin indicate the ultimate formation of MB (λ_{\max} 654 nm; Figure 5d). Oxidation of RFH₂ is rapid. Once oxidation to the flavin has taken place, then oxidation of LMB by artemisinin ensues. Very likely, rapid recycling of incipient MB, produced by oxidation of LMB by artemisinin, with the reduced flavin takes place to regenerate oxidised flavin and LMB.

7. Effect of artemisinin 1 on yeast glutathione reductase (Figure 6 and figure S2 Supporting Information): Oxidised glutathione

(GSSG, 20 mg, 3.2×10^{-2} mmol) in degassed pH 7.4 aqueous buffer (2 mL) was diluted 1:10 with degassed water to give a concentration of GSSG of 1.6×10^{-3} mmol mL⁻¹. The yeast reduced glutathione reductase solution (233 EU, 0.1 mL) was diluted to 1 mL by addition of degassed pH 7.4 aqueous buffer. The NADPH solution was prepared from NADPH (3.0 mg) and degassed pH 7.4 aqueous buffer (3 mL) to give a final concentration of 1.2×10^{-3} mmol mL⁻¹. The NADPH solution (0.4 mL, 4.8×10^{-4} mmol), the GSSG solution (0.3 mL, 4.8×10^{-4} mmol), degassed pH 7.4 buffer (1 mL) and MeCN (20 μ L) were added to a UV cuvette ($d=1$ cm) at 37 °C and treated with the yeast GR solution (0.04 mL containing 1.65 EU). The rate of NADPH turnover was followed by monitoring the decrease in absorption at λ_{\max} 340 nm for 10 min. Three experiments were carried out: 1. control, to measure the rate of NADPH decrease; 2. effect of the addition of artemisinin in MeCN solution (20 μ L containing 2.4×10^{-4} mmol artemisinin) prepared from artemisinin (7.0 mg) and MeCN (2 mL) on the rate of NADPH decrease; and 3. repetition of 2 with solutions exposed to air (Figure 6 and Supporting Information figure S2a). After 10 min, a solution (20 μ L) of di-5,5'-dithiobis-2-nitrobenzoic acid (Ellman's reagent, 29.7 mg) in methanol (25 mL) was added to the UV cuvette in order to evaluate the effect of artemisinin on the formation of reduced glutathione (GSH) under argon by monitoring absorption at λ_{\max} 412 nm; 1. control, 0.5×10^{-4} mmol mL⁻¹ GSH; 2. effect of artemisinin on GSH production, decrease to 0.35×10^{-4} mmol mL⁻¹ (Supporting Information figure S2b).

8. Comparison of the effect of artemisinin 1 on NADPH turnover in yeast glutathione reductase with NADPH turnover in the absence of artemisinin (Figure 6 and figure S3 Supporting Information): GSSG (20 mg, 3.2×10^{-2} mmol) in pH 7.4 aqueous buffer (2 mL) was diluted 1:10 with water to give a GSSG concentration of 1.6×10^{-3} mmol mL⁻¹. Yeast GR solution (147 EU, 0.1 mL) was diluted to 1 mL by addition of pH 7.4 buffer. NADPH solution was prepared from NADPH (3.0 mg) and pH 7.4 buffer (3 mL) to give a final concentration of 1.2×10^{-3} mmol mL⁻¹. The NADPH solution (0.4 mL, 4.8×10^{-4} mmol), the GSSG solution (0.3 mL, 4.8×10^{-4} mmol), and pH 7.4 buffer (1 mL) were added to the cuvette at 37 °C and treated with the yeast GR solution (0.33 EU, 0.015 mL). The rate of NADPH turnover was followed by monitoring absorption decrease at λ_{\max} 340 nm for 14 s: 1. control under argon (blue line); 2. under air (maroon line).

9. Direct comparison of the effects of artemisinin 1 on each of yeast and human recombinant glutathione reductase (figures S4 and S5, Supporting Information): All solutions were degassed. Oxidised glutathione (GSSG, 20 mg, 3.2×10^{-2} mmol) in pH 7.4 aqueous buffer (2 mL) was diluted 1:10 with water to give a concentration of GSSG of 1.6×10^{-3} mmol mL⁻¹. Yeast reduced glutathione reductase solution (147 EU, 0.1 mL) was diluted to 2 mL by the addition of pH 7.4 aqueous buffer. The NADPH solution was prepared from NADPH (3.0 mg) and pH 7.4 aqueous buffer (3 mL) to give a final concentration of 1.2×10^{-3} mmol mL⁻¹. The NADPH solution (0.4 mL, 4.8×10^{-4} mmol), the GSSG solution (0.3 mL, 4.8×10^{-4} mmol), pH 7.4 buffer (1 mL) and MeCN (20 μ L) were added to a UV cuvette ($d=1$ cm) at 37 °C and treated with the yeast GR solution (0.33 EU, 0.015 mL). The rate of NADPH turnover was followed by monitoring the decrease in absorption at λ_{\max} 340 nm from NADPH for 10 min. The experiment was carried out in triplicate, and the results are illustrated in figures S4 and S5 in the Supporting Information: 1. control; 2. effect of the addition of artemisinin in MeCN solution (20 μ L containing 2.4×10^{-4} mmol artemisinin) prepared from artemisinin (7.0 mg) and MeCN (2 mL).

GSSG (20 mg, 3.2×10^{-2} mmol) in pH 6.8 aqueous buffer (2 mL) was diluted 1:10 with water to give a concentration of GSSG of 1.6×10^{-3} mmol mL⁻¹. Recombinant human glutathione reductase solution (12 EU, 0.02 mL) was diluted to 0.5 mL by addition of pH 6.8 aqueous buffer. The NADPH solution was prepared from NADPH (3.0 mg) and pH 6.8 aqueous buffer (3 mL) to give a final concentration of 1.2×10^{-3} mmol mL⁻¹. The NADPH solution (0.4 mL, 4.8×10^{-4} mmol), the GSSG solution (0.3 mL, 4.8×10^{-4} mmol), pH 6.8 buffer (1 mL) and MeCN (20 μ L) were added to the UV cuvette at 37 °C and treated with human GR solution (0.35 EU, 0.05 mL). The rate of NADPH turnover was followed by monitoring the decrease of absorption at λ_{\max} 340 nm for 10 min. The experiment was carried out in triplicate, and the results are illustrated in figures S4 and S5, Supporting Information: 3. control; 4. effect of addition of artemisinin in MeCN solution (20 μ L containing 2.4×10^{-4} mmol artemisinin) prepared from artemisinin (7.0 mg) and MeCN (2 mL).

Electron transfer and reduction experiments

All experiments described below involving the use of each of ascorbic acid (AA) and BNAH as reductants with each of methylene blue (MB), lumiflavine (LF), and riboflavin (RF) were conducted in parallel with control experiments with artemisinins in the absence of MB, LF, and RF respectively. In each case, the blank experiment returned unreacted artemisinin.

1. Artemisinin and 9-epiartemisinin: a. Methylene blue (MB)–ascorbic acid (AA): A mixture of artemisinin (95.2 mg, 0.34 mmol), MB (25 mg, 0.20 equiv), and AA (238 mg, 4.0 equiv) in MeCN/pH 7.4 phosphate buffer (1:1, 5 mL, adjusted to pH 7.40) was stirred for 24 h, either in air or under argon in the dark. 1,3,5-Trimethoxybenzene (9.5 mg, 56.5 μ mol) was added, followed by aqueous NaHSO₄ (0.5 M, 5 mL). The mixture was treated with diethyl ether (10 mL), and the aqueous layer was separated and extracted with diethyl ether (3 \times 10 mL). The combined organic layer was washed with brine (5 mL), dried (MgSO₄), and filtered, and then concentrated under reduced pressure to leave a pale residue that was taken into CDCl₃. The solution was examined by ¹H NMR spectroscopy by using the following signals for establishing yields: artemisinin **1** δ = 5.82 ppm (H-12, singlet), deoxyartemisinin **17** δ = 5.59 ppm (H-12, singlet), and the furanoacetate **18**: δ = 6.59 ppm (singlet) against the singlet at δ = 6.08 ppm due to the aromatic protons of the standard. Yields are listed in Table 1. Additional information on the NMR method for determining yields is given in the Supporting Information. For identification of the products, the mixture from a separate reaction not containing standard was submitted to chromatography with ethyl acetate/hexanes (20:80 \rightarrow 30:70) to give artemisinin **1**, deoxyartemisinin **17** identified by comparison with an authentic sample,^[36] mp: 118–119 °C (lit.^[64] mp: 109–111 °C), and the furanoacetate **18** as a colourless solid, mp: 93–94 °C, identical with the sample obtained by ferrous-iron-catalyzed decomposition of artemisinin in our laboratory.^[9]

b. MB–BNAH: A mixture of artemisinin (93.4 mg, 0.33 mmol), MB (25 mg, 0.067 mmol, 0.2 equiv), and BNAH (287 mg, 1.34 mmol, 4 equiv) were stirred in 1:1 MeCN/pH 7.4 buffer solution (5 mL) under argon for 24 h in the dark. The mixture was treated with the standard, quenched with aqueous NaHSO₄, and extracted with diethyl ether as described above. The organic layer was washed with brine (5 mL), dried (MgSO₄), and filtered, and then concentrated under reduced pressure to leave a pale residue that was taken into CDCl₃. The solution was examined by ¹H NMR spectroscopy by using the following signals for establishing yields: artemisinin **1** δ = 5.82 ppm (H-12, singlet), deoxyartemisinin **17** δ = 5.59 ppm (H-

12, singlet), ring-opened reduction product **25** δ = 5.45 ppm (H-12, singlet) against the singlet at δ = 6.08 ppm due to the aromatic protons of the standard. Yields are listed in Table 1. The ring-opened reduction product is unstable, and undergoes spontaneous ring closure to deoxyartemisinin **17**. However, it was able to be isolated in partially purified form by rapid flash chromatography with ethyl acetate/hexanes (50:50) as a viscous gum that reverted to **17**. It is identified by spectroscopic data as follows (artemisinin numbering used throughout): ¹H NMR δ = 0.87 (d, J = 6.0 Hz, 3 H, 6-CH₃), 1.25 (d, J = 6.8 Hz, 3 H, 9-CH₃), 1.52 (s, 3 H, 3-CH₃), 3.34 (dq, J = 7.0, 4.2 Hz, 1 H, H-10), 5.45 ppm (s, 1 H, H-12); ¹³C NMR δ = 19.43, 20.56, 22.93, 25.27, 27.11, 34.74, 36.04, 36.19, 39.34, 48.32, 48.82, 87.45, 97.01, 108.30, 181.01 ppm; IR (KBr): $\tilde{\nu}_{\max}$ = 624, 868, 943, 1015, 1085, 1180, 1207, 1265, 1386, 1458, 1706 (C=O), 2874, 2937, 3422 cm⁻¹ (RCOOH); MS (CI) C₁₅H₂₄O₅ calcd for [M+1]: 285.1702; found: 285.2723; calcd for [M+1]–H₂O: 267.1596, found: 267.1555 (base peak); the peak corresponding to loss of H from the carboxylic acid at [M–1], calcd for C₁₅H₂₃O₅: 283.1545, found: 283.1546, is present.

c. Lumiflavine (LF)–BNAH: Artemisinin (47.2 mg, 0.17 mmol), LF (8.6 mg, 0.033 mmol, 0.2 equiv), and BNAH (71.7 mg, 0.33 mmol, 2 equiv) were stirred in 1:1 MeCN/pH 7.4 buffer solution (5 mL) under argon for 80 min. The standard was added to the reaction mixture that was quenched by addition of NaHSO₄ as described above. Yields of products are listed in Table 2. These were established as described above for MB–BNAH.

d. Riboflavin (RF)–BNAH: Artemisinin (95.3 mg, 0.34 mmol), RF (25.4 mg, 0.2 equiv), and BNAH (144.7 mg, 2.0 equiv) were stirred in 1:1 MeCN/phosphate buffer (5 mL, adjusted to pH 7.40) for 3 h under argon. The standard 1,3,5-trimethoxybenzene (8.3 mg, 49.35 μ mol) was added, followed by aqueous NaHSO₄ (1 M, 5 mL). The resulting mixture was worked up as described above to yield a yellow residue that was analyzed by ¹H NMR spectroscopy as described above.

e. Riboflavin (RF)–BNAH time-course experiment: In this experiment, the standard was added with the reactants at the beginning of the reaction. Artemisinin (71.1 mg, 0.252 mmol), riboflavin (19.1 mg, 0.20 equiv), BNAH (108.2 mg, 2.0 equiv), and 1,3,5-trimethoxybenzene (5.7 mg, 33.89 μ mol) were stirred in 1:1 MeCN/phosphate buffer (17.5 mL, adjusted to pH 7.40) under argon. At the first minute, ~0.7 mL of the reaction mixture was withdrawn and immediately added to aqueous NaHSO₄ (1 M, 1 mL); 1 mL diethyl ether was employed to dilute the extract. The aqueous layer was separated and extracted with diethyl ether (3 \times 1 mL). The combined organic layer was washed with aqueous NaHSO₄ (1 M, 2 mL), followed by brine (2 mL), and then dried (MgSO₄). After filtration, the solution was concentrated under reduced pressure, and the residue was taken into CDCl₃ and the ¹H NMR spectrum was obtained. The steps were repeated at 30, 60, 90, 120, 150, and 180 min. Under these conditions, the progressive formation of each of the open ring-opened reduction product **25** and deoxyartemisinin **17** was easily followed. The appearance of a signal in the ¹H NMR spectrum at δ = 5.65 ppm has yet to be assigned. It is not possible to isolate any product containing such a signal after chromatography of the reaction mixture as described in b. above. Additional information and figures are given in the Supporting Information.

f. Riboflavin (RF)–MB–BNAH: Artemisinin (47.8 mg, 0.169 mmol), RF (12.8 mg, 0.2 equiv), methylene blue (12.6 mg, 0.2 equiv), and BNAH (72.4 mg, 2.0 equiv) were stirred in 1:1 MeCN/phosphate buffer (1:1, 5 mL, adjusted to pH 7.4) for 1.5 h under argon. 1,3,5-Trimethoxybenzene (4.9 mg, 29.13 μ mol) and solid NaHSO₄·H₂O

(707.5 mg, 5.12 mmol) were added, followed by diethyl ether (10 mL). The aqueous layer was separated and extracted with diethyl ether (3×5 mL). The combined organic layer was washed with aqueous NaHSO₄ (1 M, 10 mL) followed by brine (10 mL), and then dried (MgSO₄). After filtration, the solution was evaporated under reduced pressure to leave a residue that was analyzed by ¹H NMR spectroscopy. The signal due to the proton at H-10 (singlet) was used for establishing yields: artemisinin **1** δ = 5.85 ppm, deoxyartemisinin **17** δ = 5.69 ppm, 9-epideoxyartemisinin **17e** δ = 5.66 ppm, and ring-opened carboxylic acid **25** δ = 5.45 ppm. The residue was shown to consist of artemisinin **1** (27%) and the following products (yields based on reacting artemisinin): deoxyartemisinin **17** (21%), 9-epideoxyartemisinin **17e** (6%), and the ring-opened carboxylic acid **25** (53%).

The reaction was repeated precisely under the foregoing conditions and time (1.5 h), but in the absence of MB. The product mixture consisted of artemisinin **1** (28%) and the following products (yields based on reacting artemisinin): deoxyartemisinin **17** (29%), 9-epideoxyartemisinin **17e** (5%), and the ring-opened carboxylic acid **25** (45%).

g. FMN-BNAH: Artemisinin (47 mg, 0.17 mmol), FMN (22.8 mg, 0.20 equiv), and BNAH (72.1 mg, 2.0 equiv) were stirred in MeCN/phosphate buffer (1:1, 5 mL, adjusted to pH 7.4) under argon for 3 h. 1,3,5-Trimethoxybenzene (4.5 mg, 26.8 μmol) and then solid NaHSO₄·H₂O (730 mg, 5.29 mmol) were added, followed by diethyl ether (10 mL). The aqueous layer was separated and extracted with diethyl ether (3×5 mL). The combined organic layer was washed with aqueous NaHSO₄ (1 M, 10 mL) followed by brine (10 mL), and then dried (MgSO₄). The solution was then concentrated under reduced pressure to leave a residue that was analyzed by ¹H NMR spectroscopy as described above.

h. FAD-NADPH: A mixture of artemisinin (14.3 mg, 50.65 μmol), FAD (8.4 mg, 0.20 equiv), and NADPH (49.9 mg, 1.2 equiv) were stirred in MeCN/phosphate buffer (1:1, 1.5 mL, adjusted to pH 7.4) under argon for 3 h. 1,3,5-Trimethoxybenzene (2.4 mg, 14.27 μmol) and solid NaHSO₄·H₂O (147.0 mg, 1.065 mmol) were then added. Diethyl ether (3 mL) was employed to dilute the reaction mixture. The aqueous layer was separated and extracted with diethyl ether (3×2 mL). The combined organic layer was washed with aqueous NaHSO₄ (1 M, 3 mL) and brine (3 mL), and then dried (MgSO₄). The ether was evaporated under reduced pressure to leave a pale-yellow residue that was analyzed for the presence of each of artemisinin **1** and the reduction products **17** and **25** by ¹H NMR spectroscopy as described above.

i. Artemisinin-reduced glutathione (GSH): Artemisinin (47.1 mg, 0.17 mmol) and GSH (104.5 mg, 0.34 mmol, 2.0 equiv) were stirred in 1:1 MeCN/pH 7.4 buffer solution (5 mL) under argon for 24 h. The standard 1,3,5-trimethoxybenzene was added to the reaction mixture that was quenched by addition of NaHSO₄ as described above. Diethyl ether (10 mL) was added to the mixture. The aqueous layer was separated and extracted with diethyl ether (3×5 mL). The combined organic layer was washed with aqueous NaHSO₄ (1 M, 10 mL) followed by brine (10 mL), and then dried (MgSO₄). After filtration, the solution was evaporated under reduced pressure to leave a residue that was analyzed by ¹H NMR spectroscopy. This showed the presence of artemisinin (98.5%).

9-Epiartemisinin: *a1. RF-BNAH:* 9-Epiartemisinin **1e** (47.6 mg, 0.169 mmol), RF (12.6 mg, 0.20 equiv), and BNAH (72.3 mg, 2.0 equiv) were stirred in MeCN/phosphate buffer (1:1, 5 mL, adjusted to pH 7.4) under argon for 3 h. 1,3,5-Trimethoxybenzene (3.7 mg, 22 μmol) and then solid NaHSO₄·H₂O (715 mg, 5.18 mmol)

were added to the mixture, followed by diethyl ether (10 mL). The aqueous layer was separated and extracted with diethyl ether (3×5 mL). The combined organic layer was washed with aqueous NaHSO₄ (1 M, 10 mL) and brine (10 mL) and then dried (MgSO₄). After filtration, the solution was evaporated under reduced pressure to leave a residue that was analyzed by ¹H NMR spectroscopy by using the following signals for establishing yields: 9-epiartemisinin **1a** δ = 5.92 ppm (H-12, singlet), 9-epideoxyartemisinin **17e** δ = 5.751 ppm (H-12, singlet), ring-opened reduction product **25e** δ = 5.30 ppm (singlet), and a formate ester δ = 8.186 ppm (doublet, *J* = 0.4 Hz). The experiment was repeated without internal standard. Flash chromatography of the residue over silica gel with ethyl acetate/hexanes (20:80) gave 9-epiartemisinin **1e** and 9-epideoxyartemisinin **17e**. With ethyl acetate/hexanes (50:50) a small amount of a compound believed to be a formate ester and then the ring-opened reduction product **25e** were obtained. The 9-epideoxyartemisinin **17e** was obtained as fine white needles, mp: 130–132 °C. ¹H NMR: δ = 0.92 (d, *J* = 5.6 Hz, 3H, 6-CH₃), 1.10–1.40 (m, 4H), 1.47 (d, *J* = 8.0 Hz, 3H, 9-CH₃), 1.51 (s, 3H, 3-CH₃), 1.55–1.63 (m, 2H), 1.71–1.78 (m, 3H), 1.86–1.90 (m, 1H), 1.94 (dd, *J* = 13.6, 3.6 Hz, 1H), 2.34–2.40 (dq, *J* = 15.2, 7.6 Hz, 1H, 9-H), 5.75 ppm (s, 1H, H-12); ¹³C NMR δ = 19.33, 20.88, 22.76, 24.83, 31.90, 34.43, 34.72, 36.14, 40.27, 42.87, 45.50, 82.90, 100.59, 110.22, 173.48 ppm; IR (KBr): $\tilde{\nu}_{\max}$ = 1741 cm⁻¹ (C=O); MS (CI) C₁₅H₂₂O₄ calcd for [M+1]: 267.1596, found: 267.1598.

The unknown compound, likely a formate ester, was obtained as an amorphous white solid. ¹H NMR: δ = 0.90 (d, *J* = 6.0 Hz, 3H, 6-Me), 1.12 (d, *J* = 7.2 Hz, 3H, 9-Me), 1.47 (s, 3H, 3-Me), 2.20–2.26 (m, 1H), 3.16–3.23 (m, 1H), 6.35 (s, 1H, H-12), 8.19 ppm (d, *J* = 0.4 Hz, 1H, -CHO?); ¹³C NMR δ = 16.93, 19.34, 23.09, 24.15, 25.34, 34.28, 35.93, 36.25, 38.30, 47.17, 47.86, 87.57, 95.57, 110.07, 161.01, 183.35 ppm; IR (KBr): $\tilde{\nu}_{\max}$ = 1712.9, 1736.3 cm⁻¹.

The ring-opened reduction product **25e** was obtained as a viscous unstable gum, that reverted to 9-epideoxyartemisinin **17e** on standing. ¹H NMR: δ = 0.86 (d, *J* = 6.4 Hz, 3H, 6-Me), 1.13 (d, *J* = 6.8 Hz, 3H, 9-Me), 1.39 (s, 3H, 3-Me), 2.73–2.81 (m, 1H), 5.30 ppm (s, 1H, H-12); ¹³C NMR δ = 17.65, 19.45, 22.91, 24.04, 27.08, 34.72, 35.73, 35.92, 40.47, 47.91, 49.64, 87.43, 98.18, 107.33, 185.01 ppm; IR (KBr): $\tilde{\nu}_{\max}$ = 3413 (COOH), 1698 cm⁻¹ (C=O). The peak corresponding to the molecular ion could not be found in the mass spectrum; the base peak corresponds to [M+1]–H₂O: MS (CI) C₁₅H₂₄O₅ calcd for [M+1]: 285.1702; calcd for [M+1]–H₂O: 267.1596, found: 267.1584; the peak corresponding to loss of H from the carboxylic acid at [M–1], calcd for C₁₅H₂₃O₅: 283.1545, found: 283.1541, is present.

a2. Control: A control experiment was carried out as follows. 9-Epiartemisinin **1e** (47.6 mg, 0.169 mmol) and BNAH (72.1 mg, 2.0 equiv) were stirred in MeCN/phosphate buffer (1:1, 5 mL, adjusted to pH 7.40) for 3 h in argon. 1,3,5-Trimethoxybenzene (3.7 mg, 22 μmol) and NaHSO₄·H₂O (724 mg, 5.24 mmol) were added, followed by diethyl ether (10 mL). Workup was carried out as described above to give a residue, the analysis of which by ¹H NMR spectroscopy indicated the presence of 9-epiartemisinin **1e** (98%) and artemisinin **1**, δ = 5.85 (H-12, singlet) (2%).

2. Dihydroartemisinin (DHA): *a. MB-AA:* DHA **2** (96.4 mg, 0.34 mmol), MB (26 mg, 0.2 equiv), and AA (238 mg, 4.0 equiv) were stirred in MeCN/phosphate buffer (1:1, 5 mL, adjusted to pH 7.4) for 24 h, either under air or argon. 1,3,5-Trimethoxybenzene (11.8 mg, 70.2 μmol) was added, followed by aqueous NaHSO₄ (0.5 M, 5 mL). The mixture was treated with diethyl ether (10 mL), and the aqueous layer was separated and extracted with diethyl

ether (3 × 10 mL). The combined organic layer was washed with brine (5 mL), dried (MgSO₄), and filtered, and then concentrated under reduced pressure to leave a pale residue that was taken into CDCl₃. The solution was examined by ¹H NMR spectroscopy by using the following signals for establishing yields: DHA **2** δ = 5.37 ppm (singlet) and 5.595 ppm (singlet) for each of the α and β epimers, deoxyDHA **19** δ = 5.28 ppm (singlet) and 5.32 ppm (singlet) for each of the α and β epimers, tricarbonyl compound **20** δ = 9.72 ppm (doublet), furanodicarbonyl compound **21** δ = 9.91 ppm (singlet). For identification of the products, the mixture from a separate reaction not containing standard was submitted to chromatography with ethyl acetate/hexanes (10:90 → 40:60) to give the tricarbonyl and furanodicarbonyl compounds **20** and **21** as oils identical with samples previously prepared in our laboratory,^[8,9,11] and deoxyDHA **19**, fine needles, mp: 142–144 °C (lit.^[61] mp: 142–143 °C), identical with an authentic sample prepared by hydrogenation of DHA according to the published method.^[61]

b1. MB–BNAH: DHA (95 mg, 0.334 mmol), MB (25 mg, 0.067 mmol, 0.2 equiv), and BNAH (286.9 mg, 1.34 mmol, 4 equiv) in MeCN/pH 7.4 buffer (1:1, 5 mL) was stirred under argon. After 24 h, 1,3,5-trimethoxybenzene (9.5 mg, 0.056 mmol) was added as internal NMR standard followed by aqueous NaHSO₄ (0.5 M, 5 mL). Diethyl ether (10 mL) was added, the aqueous layer was separated, and the latter extracted with further portions of diethyl ether (3 × 10 mL). The combined organic layer was washed with brine (5 mL), then dried over MgSO₄. After filtration and concentration of the filtrate under reduced pressure, the residue was taken into CDCl₃. ¹H NMR spectroscopic measurements were conducted as described above. For estimation of the yield of 9-epideoxyDHA **19e**, the doublet at δ = 5.03 due to H-10 was used. In order to isolate and characterise the 9-epideoxyDHA **19e**, the following reaction was carried out. DHA (190 mg, 0.67 mmol), MB (50 mg, 0.13 mmol, 0.2 equiv), and BNAH (574 mg, 2.68 mmol, 4 equiv) were stirred in the 1:1 MeCN/pH 7.4 buffer solution (10 mL) under argon for 24 h. The mixture was treated with solid NaHSO₄·H₂O (1.6 g) and extracted with diethyl ether (3 × 15 mL). The combined organic extract was washed with brine (30 mL) and dried (MgSO₄). The solvent was evaporated under reduced pressure, and the residue was submitted to flash chromatography with ethyl acetate/hexanes (35:65) to give the product that was recrystallised from ethyl acetate to give **19e** (63.5 mg) as colourless bars, mp: 144–145 °C; ¹H NMR: δ = 0.88 (3H, d, *J* = 6.0 Hz, 6-Me), 1.12 (3H, d, *J* = 6.8 Hz, 9-Me), 1.16–1.46 (5H, m), 1.50 (3H, s, 3-Me), 1.56–1.74 (6H, m), 1.82–1.87 (1H, m), 2.80 (1H, d, *J* = 6 Hz, -OH), 5.03 (1H, dd, *J* = 7.6, 6 Hz, H-10), 5.41 ppm (1H, s, H-12); ¹³C NMR: δ = 18.01, 18.89, 21.33, 23.04, 32.05, 33.76, 33.80, 34.45, 40.93, 43.48, 44.50, 81.91, 93.75, 96.64, 106.45 ppm; MS (ESI) C₁₅H₂₄O₄ calcd for [M+1]: 269.1753, found: 269.1765; calcd for [(M+1)–H₂O]: 251.1647, found: 251.1647 (base peak).

b2. BNAH (control): DHA (190 mg, 0.67 mmol) and BNAH (576 mg, 2.7 mmol, 4 equiv) in MeCN/pH 7.4 buffer (1:1, 10 mL) was stirred under argon. After 24 h, the mixture was treated with aqueous NaHSO₄ (0.5 M, 10 mL). Diethyl ether (20 mL) was added, the aqueous layer was separated, and the latter extracted with further portions of diethyl ether (3 × 20 mL). The combined organic layer was washed with brine (5 mL), then dried over MgSO₄. After filtration and concentration of the filtrate under reduced pressure, the residue was submitted to flash chromatography with ethyl acetate/hexanes (30:70) to give the product as a viscous pale-yellow oil. The ¹H NMR spectrum indicated the presence of a 2:1 mixture of epimers of **26**. ¹H NMR (major epimer): δ = 0.74 (d, *J* = 6.8 Hz, 1H), 0.83 (d, *J* = 7.6 Hz, 3H, 6-Me), 0.92 (d, *J* = 6 Hz, 3H, 9-Me), 1.08–1.18

(m, 2H), 1.18–1.45 (m, 5H), 1.53–1.79 (m, 6H), 1.79–2.08 (m, 7H), 2.13 (s, 3H, COCH₃), 2.24–2.34 (m, 1H), 2.43–2.68 (m, 3H), 5.07 (s, 1H, H-10), 10.28 ppm (s, 1H, CHO); ¹H NMR (minor epimer): δ = 0.74 (d, *J* = 6.8 Hz, 1H), 0.83 (d, *J* = 7.6 Hz, 3H, 9-Me), 0.92 (d, *J* = 6 Hz, 3H, 6-Me), 1.08–1.18 (m, 2H), 1.18–1.45 (m, 5H), 1.53–1.79 (m, 6H), 1.79–2.08 (m, 7H), 2.13 (s, 3H, COCH₃), 2.24–2.34 (m, 1H), 2.43–2.68 (m, 3H), 5.067 (s, 1H, H-10), 10.17 ppm (s, 1H, CHO). The product is matched directly with the authentic sample obtained by thermal decomposition of DHA.^[36]

c1. BNAH–LF: A mixture of DHA (47.5 mg, 0.17 mmol), LF (8.6 mg, 0.033 mmol, 0.2 equiv), and BNAH (71.7 mg, 0.33 mmol, 2.0 equiv) in MeCN/pH 7.5 aqueous buffer (5 mL) was stirred under argon for 80 min. After addition of standard and aqueous NaHSO₄ as described for the corresponding reaction involving artemisinin, the mixture was worked up to give a pale-yellow residue that was analyzed by ¹H NMR spectroscopy as described in the DHA–MB–BNAH experiment above.

c2. Peroxyhemiacetal **26–BNAH–LF:** A mixture of the peroxyhemiacetal **26** (54 mg, 0.19 mmol), LF (9.8 mg, 0.04 mmol, 0.2 equiv), and BNAH (81.4 mg, 0.38 mmol, 2.0 equiv) in 1:1 MeCN/pH 7.4 buffer 1:1 was stirred under argon for 80 min. Addition of standard and aqueous NaHSO₄ was followed by workup as described above to leave a residue, the examination of which by ¹H NMR spectroscopy revealed the presence of each of the reduction products **19** and **19e**, and the tricarbonyl compound **20** (Table 2).

d. RF–BNAH: A mixture of DHA (96.0 mg, 0.34 mmol), RF (25.4 mg, 0.2 equiv) and BNAH (145.5 mg, 0.68 mmol, 2.0 equiv) in MeCN/phosphate buffer (1:1, 5 mL, adjusted to pH 7.4) was stirred under argon for 3 h. 1,3,5-Trimethoxybenzene (8.3 mg, 49.35 μmol) and solid NaHSO₄·H₂O (458 mg, 3.32 mmol) were added, followed by diethyl ether (10 mL). The aqueous layer was separated and extracted with diethyl ether (3 × 5 mL). The combined organic layer was washed with aqueous NaHSO₄ (1 M, 10 mL), and then brine (10 mL). It was dried (MgSO₄), filtered, and concentrated under reduced pressure. The pale residue was analyzed by ¹H NMR spectroscopy, that showed the presence solely of 9-epideoxyDHA **19e** (H-10; δ = 5.03) (77%).

3. Artemether: **a. MB–AA:** Artemether (101 mg, 0.34 mmol), MB (25 mg, 0.20 equiv) and AA (236 mg, 4.0 equiv) were stirred in MeCN/phosphate buffer (1:1, 5 mL, adjusted to pH 7.4 for 24 h under air or argon. 1,3,5-Trimethoxybenzene (9.0 mg, 53.5 μmol) was added, followed by aqueous NaHSO₄ (0.5 M, 5 mL). The mixture was processed as described above, and the residue analyzed by ¹H NMR spectroscopy by using the following signals for establishing yields: artemether **3** δ = 5.36 ppm (singlet), furanoacetate **22** 6.21 ppm (singlet), 4-hydroxydeoxyartemether **23** 5.24 ppm (singlet), tricarbonyl compound **20** 9.71 ppm (singlet), and the furanodicarbonyl compound **21** 9.91 ppm (singlet). A further signal at δ = 8.08 ppm (singlet) is evident in the NMR spectrum, and this is tentatively ascribed to a formate ester; attempts to isolate the compound by chromatography were not successful; the amount present is ~4%. The other products were isolated by chromatography with ethyl acetate/hexanes (10:90 → 40:60) and identified as described above, or according to published data. The furanoacetate **22** is identified by comparison with a sample obtained by ferrous-iron-induced decomposition of artemether.^[11] It was obtained as white rectangular shaped crystals, mp: 93–94 °C (lit.^[11] mp: 96–97 °C); ¹H NMR δ = 0.88 (d, *J* = 7.2 Hz, 6-Me), 0.92 (d, *J* = 6.4 Hz, 9-Me), 1.27–1.36 (m, 1H), 1.47–1.51 (m, 1H), 1.60–1.66 (m, 2H), 1.76–1.97 (m, 5H), 2.12 (s, -OCOMe), 2.35–2.43 (m, 1H), 3.41 (s, -OMe), 3.88–3.94 (ddd, *J* = 8.2, 8.2, 7.6 Hz, 1H, H4), 4.23–4.28 (ddd, *J* = 9.6,

8.0, 2.0 Hz, 1H, H-4), 4.61–4.62 (d, $J=4$ Hz, 1H), 6.23 ppm (s, 1H, H-12); ^{13}C NMR: $\delta=13.11, 21.21, 22.33, 25.40, 28.43, 31.29, 34.06, 36.53, 47.67, 56.33, 56.64, 69.29, 81.24, 88.87, 104.09, 170.00$ ppm; MS (CI) $\text{C}_{16}\text{H}_{26}\text{O}_5$ calcd for $[M]^+$: 298.1780, found: 298.1777; calcd for $[M+1]$: 299.1858, found: 299.1801; calcd for $[M+1]-\text{MeOH}$: 267.1596, found: 267.1587. 4-Hydroxy-2-deoxyartemether **23** was obtained as an oil. It has been previously characterized as needles, mp: 65–67 °C.^[11] However, spectroscopic data match that previously reported; ^1H NMR spectrum $\delta=0.85$ (d, $J=6.4$ Hz, 6-Me), 0.90 (d, $J=7.6$ Hz, 9-Me), 1.55 (s, 3-Me), 2.42–2.46 (m, 1H), 3.37 (s, -OMe), 3.55–3.56 (m, 1H, H-4), 4.62 (d, $J=4.0$ Hz, 1H, H-10), 5.25 ppm (s, 1H, H-12); ^{13}C NMR $\delta=12.98, 19.49, 21.68, 25.65, 30.98, 31.05, 35.38, 35.45, 41.36, 43.15, 56.73, 70.25, 84.82, 94.15, 102.17, 108.57$ ppm; MS (CI) $\text{C}_{16}\text{H}_{26}\text{O}_5$ calcd for $[M]^+$: 298.1780, found: 298.1742; calcd for $[M+1]$: 299.1858, found: 299.1806; calcd for $[M+1]-\text{H}_2\text{O}$: 281.3673, found: 281.1762; calcd for $[M+1]-\text{MeOH}$: 267.1596, found: 267.1599; 238.1574 (100).

b. *LF-BNAH*: A mixture of artemether (49.9 mg, 0.17 mmol), LF (8.6 mg, 0.03 mmol, 0.2 equiv), and BNAH (71.7 mg, 0.33 mmol, 2.0 equiv) in MeCN/pH 7.4 buffer (5.0 mL) under argon was stirred for 2.5 h, and then treated with standard and aqueous NaHSO_4 as described for the corresponding reaction involving artemisinin. Workup gave a pale residue that was analyzed by ^1H NMR spectroscopy as described in the DHA–MB–BNAH experiment above.

c. *RF-BNAH*: Artemether (99.9 mg, 0.33 mmol), RF (25.1 mg, 0.2 equiv), and BNAH (144.2 mg, 2.0 equiv) were stirred in MeCN/phosphate buffer (1:1, 5 mL, adjusted to pH 7.40) under argon for 3 h. 1,3,5-Trimethoxybenzene (7.2 mg, 42.8 μmol), solid NaHSO_4 (994 mg, 7.2 mmol), and diethyl ether (10 mL) were added sequentially. The aqueous layer was separated and extracted with diethyl ether (3 \times 5 mL). The combined organic layer was washed with aqueous NaHSO_4 (1 M, 10 mL), brine (10 mL), and then dried (MgSO_4). The solution was filtered and concentrated under reduced pressure. The residue was analyzed by ^1H NMR spectroscopy as described above by using the signals for 9-epideoxyDHA **19e** at $\delta=5.03$ ppm (doublet), deoxyDHA 5.34 ppm (singlet) and 5.364 ppm (singlet) for each of the α and β epimers, respectively, and for the tricarbonyl compound **20** at 9.73 ppm (doublet). Approximately 3% of another compound, apparently a formate ester, with a signal at $\delta=8.08$ ppm (singlet), was present in the product mixture, but could not be isolated.

4. Artesunate: a1. *MB-AA*: Artesunate (130 mg, 0.34 mmol), MB (25.5 mg, 0.20 equiv) and AA (238 mg, 4.0 equiv) were stirred in MeCN/phosphate buffer (1:1, 5 mL, adjusted to pH 7.4) under air or argon for 24 h. 1,3,5-Trimethoxybenzene (6.8 mg, 40 μmol) was added, followed by aqueous NaHSO_4 (0.5 M, 5 mL) and diethyl ether (5 mL). The mixture was processed as described for the DHA reaction above, and the residue was analyzed by ^1H NMR spectroscopy by using the following signals for establishing yields: artesunate **4** $\delta=5.41$ ppm (singlet) and the furanoacetate **24** 6.18 ppm (singlet). A small amount of another product, designated as a formate ester with a signal at $\delta=8.04$ ppm was also present (~3%) in the product mixture. However, this product could not be isolated. The furanoacetate **24** was isolated after chromatography of the mixture and elution with ethyl acetate/hexanes (25:75) as a colourless oil, the spectroscopic data of which are in accord with those of an authentic sample previously prepared in our laboratory^[9] and as reported.^[11]

a2. *AA (control)*: To establish if artesunate undergoes hydrolysis to DHA under the reaction conditions,^[36] the following control experiment was carried out. Artesunate (130 mg, 0.34 mmol) and AA

(238 mg, 4.0 equiv) were stirred in MeCN/phosphate buffer (1:1, 5 mL, adjusted to pH 7.40) under air for 24 h. 1,3,5-Trimethoxybenzene (10.1 mg, 60.05 μmol) was added, and the mixture was worked up as described above to leave a crystalline residue. Analysis by ^1H NMR spectroscopy using the signal at $\delta=5.412$ ppm (singlet, H-10) indicated that it consisted solely of artesunate (99.2% recovery).

b. *FAD-NADPH*: Artesunate (12.9 mg, 33.56 μmol), FAD (5.7 mg, 0.2 equiv), and NADPH (56.3 mg, 2.0 equiv) were stirred in phosphate buffer (1 mL, adjusted to pH 7.40) under argon for 3 h. 1,3,5-Trimethoxybenzene (2.5 mg, 14.86 μmol) and solid $\text{NaHSO}_4 \cdot \text{H}_2\text{O}$ (168.9 mg, 1.223 mmol) were added, and the resulting mixture was treated with diethyl ether (2 mL). The aqueous layer was separated and extracted with diethyl ether (3 \times 2 mL). The combined organic layer was washed with 4 mL aqueous NaHSO_4 (1 M, 4 mL) and then brine (4 mL). The organic solution was dried over MgSO_4 , then filtered and concentrated by evaporation under reduced pressure. The residue was analyzed by ^1H NMR spectroscopy by using the peaks due to artesunate at $\delta=5.43$ ppm (singlet), deoxyDHA **19** at 5.345 ppm (singlet) and 5.365 ppm (singlet) for each of the α and β epimers, respectively, the tricarbonyl compound **20** at $\delta=9.734$ ppm (singlet), and a second compound believed to be a formate ester at $\delta=8.065$ ppm (singlet). As in a1 above, the last compound could not be isolated, but the amount present is estimated to be 5%. It likely converts into the tricarbonyl compound **20** during chromatography.

5. Artemisone: a1. *MB-AA*: Artemisone (134.5 mg, 0.335 mmol), MB (25.4 mg, 0.2 equiv), and AA (237 mg, 4.0 equiv) were stirred in MeCN/phosphate buffer (1:1, 5 mL, adjusted to pH 7.4) under air or argon for 24 h. 1,3,5-Trimethoxybenzene (12.1 mg, 71.94 μmol) was added, followed by aqueous NaHSO_4 (0.5 M, 5 mL), and then diethyl ether (5 mL). The aqueous layer was separated and extracted with diethyl ether (3 \times 3 mL). The combined organic layer was washed with brine (5 mL), dried (MgSO_4), and then filtered and concentrated by evaporation under reduced pressure to leave a residue that was analyzed by ^1H NMR spectroscopy by using the following signals for establishing yields: artemisone **5** $\delta=5.275$ ppm (singlet), tricarbonyl compound **20** 9.71 ppm (singlet), and furanodicarbonyl compound **21** 9.91 ppm (singlet).

a2. *AA (control)*: To establish if artemisone undergoes hydrolysis under the reaction conditions to DHA, the following control experiment was carried out. Artemisone (135 mg, 0.34 mmol) and AA (238 mg, 4.0 equiv) were stirred in MeCN/phosphate buffer (1:1, 5 mL, adjusted to pH 7.4) under air for 24 h. 1,3,5-Trimethoxybenzene (11.1 mg, 66.00 μmol) was added, and the reaction mixture was worked up as described above to leave a residue, the analysis of which by ^1H NMR spectroscopy revealed the presence of artemisone ($\delta=5.257$ ppm; singlet, H-10) (96.4% recovery).

b. *LF-BNAH*: Artemisone (67.1 mg, 0.167 mmol), LF (8.6 mg, 0.033 mmol, 0.2 equiv), and BNAH (71.7 mg, 0.34 mmol, 2.0 equiv) in MeCN/pH 7.4 buffer (1:1, 5.0 mL) were stirred under argon for 6 h. After addition of the standard 1,3,5-trimethoxybenzene (3.6 mg) and solid $\text{NaHSO}_4 \cdot \text{H}_2\text{O}$ (500 mg), the reaction mixture was diluted with diethyl ether (10 mL). The aqueous layer was separated and extracted with diethyl ether (3 \times 5 mL). The combined organic layer was washed with aqueous NaHSO_4 (1 M, 10 mL), followed by brine (10 mL). After drying (MgSO_4), the organic solvent was evaporated under reduced pressure to leave a residue that was analyzed by ^1H NMR spectroscopy using the following signals for establishing yields: artemisone **5** $\delta=5.267$ ppm (singlet, H-10), 9-epideoxyDHA **19e** 5.01 (doublet, H-10), deoxyDHA **19** 5.33 ppm

(singlet, H-10), and 5.35 ppm (singlet, H-10) for each of the α and β epimers, respectively, and tricarbonyl compound **20** 9.719 ppm (singlet, CHO).

c. *RF-BNAH*: Artemisone (135 mg, 0.34 mmol), RF (25 mg, 0.20 equiv), and BNAH (144 mg, 2.0 equiv) were stirred in MeCN/phosphate buffer (1:1, 5 mL, adjusted to pH 7.4) under argon for 3 h. 1,3,5-Trimethoxybenzene (7.3 mg, 43.4 μ mol) and solid NaH-SO₄·H₂O (1.002 g, 7.26 mmol) were added, followed by diethyl ether (10 mL). The aqueous layer was separated and extracted with diethyl ether (3×5 mL). The combined organic layer was washed with aqueous NaHSO₄ (1 M, 10 mL), followed by brine (10 mL). After drying (MgSO₄), the organic solvent was evaporated under reduced pressure to leave a residue that was analyzed by ¹H NMR spectroscopy using the signals for establishing yields as described above.

Acknowledgements

Work at HKUST was carried out in the Open Laboratory of Chemical Biology of the Institute of Molecular Technology for Drug Discovery and Synthesis with financial support from the Government of the HKSAR University Grants Committee Areas of Excellence Fund (Project Nos. AoE P/10-01/01-02-I, AOE/P-10/01-2-II) and the University Grants Council (Grant Nos. HKUST 6493/06M and 600507). The Milan work was conducted partly in the context of the AntiMal project, funded under the 6th Framework Programme of the European Community (Contract No. IP-018834) to D.M. The authors are solely responsible for its content, it does not represent the opinion of the European Community and the Community is not responsible for any use that might be made of the information contained therein. The financial support of the University of Milan (FIRB reti 2005RBPR05NWWC) is also acknowledged.

Keywords: artemisinins • flavins • flavoenzymes • malaria • oxidative stress

- J.-F. Zhang, *A Detailed Chronological Record of Project 523 and The Discovery and Development of Qinghaosu (Artemisinin)*, Yang Cheng Evening News Publishing Company, Yang Cheng (China), **2005**.
- R. T. Eastman, D. A. H. Fidock, *Nat. Rev. Microbiol.* **2009**, *7*, 864–874.
- R. K. Haynes, B. Fugmann, J. Stetter, K. Rieckmann, H.-D. Heilmann, H.-W. Chan, M.-K. Cheung, W.-L. Lam, H.-N. Wong, S. L. Croft, L. Vivas, L. Rattray, L. Stewart, W. Peters, B. L. Robinson, M. D. Edstein, B. Kotecka, D. E. Kyle, B. Beckermann, M. Gerisch, M. Radtke, G. Schmuck, W. Steinke, U. Wollborn, K. Schmeer, A. Römer, *Angew. Chem.* **2006**, *118*, 2136–2142; *Angew. Chem. Int. Ed.* **2006**, *45*, 2082–2088.
- a) T. N. C. Wells, P. L. Alonso, W. E. Gutteridge, *Nat. Rev. Drug Discovery* **2009**, *8*, 879–891; b) S. H. I. Kappe, A. M. Vaughan, J. A. Boddey, A. F. Cowman, *Science* **2010**, *328*, 862–866.
- P. M. O'Neill, J. Chadwick, S. L. Rawe, in *Chemistry of Peroxides* Vol. 2, Pt. 2 (Ed.: Z. Rappoport), Wiley, Chichester (UK), **2006**, pp. 1279–1346.
- P. M. O'Neill, V. E. Barton, S. A. Ward, *Molecules* **2010**, *15*, 1705–1721.
- A. Robert, F. Benoit-Vicala, B. Meunier, *Coord. Chem. Rev.* **2005**, *249*, 1927–1936.
- R. K. Haynes, W.-Y. Ho, H.-W. Chan, B. Fugmann, J. Stetter, S. L. Croft, L. Vivas, W. Peters, B. L. Robinson, *Angew. Chem.* **2004**, *116*, 1405; *Angew. Chem. Int. Ed.* **2004**, *43*, 1381–1385.
- R. K. Haynes, W.-C. Chan, C.-M. Lung, A. C. Uhlemann, U. Eckstein, D. Taramelli, S. Parapini, D. Monti, S. Krishna, *ChemMedChem* **2007**, *2*, 1480–1497.
- P. Coghi, N. Basilico, D. Taramelli, W.-C. Chan, R. K. Haynes, D. Monti, *ChemMedChem* **2009**, *4*, 2045–2053.
- W.-M. Wu, Y. Wu, Y.-L. Wu, Z.-J. Yao, C. M. Zhou, Y. Li, F. Shan, *J. Am. Chem. Soc.* **1998**, *120*, 3316–3325.
- U. Eckstein-Ludwig, R. J. Webb, I. D. A. Van Goethem, J. M. East, A. G. Lee, M. Kimura, P. M. O'Neill, P. G. Bray, S. A. Ward, S. Krishna, *Nature* **2003**, *424*, 957–961.
- F. B. Garah, J.-L. Stigliani, F. Coslédan, B. Meunier, A. Robert, *ChemMedChem* **2009**, *4*, 1469–1479.
- W. Ittarat, A. Sreepian, A. Srisarin, K. Pathepochitvong, *Southeast Asian J. Trop. Med. Public Health* **2003**, *34*, 744–750.
- S. R. Krungkrai, Y. Yuthavong, *Trans. R. Soc. Trop. Med. Hyg.* **1987**, *81*, 710–714.
- T. Efferth, *Current Drug Targets* **2006**, *7*, 407–421.
- R. K. Haynes, G. Schmuck, *Antimicrob. Agents Chemother.* **2002**, *46*, 821–827.
- M. A. Avery, F.-L. Gao, W. K. M. Chong, S. Mehrotra, W. K. Milhous, *J. Med. Chem.* **1993**, *36*, 4264–4275.
- a) J. L. Vennerstrom, M. T. Makler, C. K. Angerhofer, J. A. Williams, *Antimicrob. Agents Chemother.* **1995**, *39*, 2671–2677; b) H. Atamna, M. Krugliak, G. Shalmiev, E. Deharo, G. Pescarmona, H. Ginsburg, *Biochem. Pharmacol.* **1996**, *51*, 693–700.
- A. Zougrana, B. Coulibaly, A. Sié, I. Walter-Sack, F. P. Mockenhaupt, B. Kouyaté, R. H. Schirmer, C. Klose, U. Mansmann, P. Meissner, O. Müller, *PLoS ONE* **2008**, *3*, e1630.
- M. Akoachere, K. Buchholz, E. Fischer, J. Burhenne, W. E. Haefeli, R. H. Schirmer, K. Becker, *Antimicrob. Agents Chemother.* **2005**, *49*, 4592–4597.
- P. Grellier, J. Šarlauskas, Ž. Anusevičius, A. Marozienė, C. Houee-Levin, J. Schrevel, N. Čėnas, *Arch. Biochem. Biophys.* **2001**, *393*, 199–206.
- K. Becker, S. Rahlfs, C. Nickel, R. H. Schirmer, *Biol. Chem.* **2003**, *384*, 551–566.
- K. Buchholz, R. H. Schirmer, J. K. Eubel, M. B. Akoachere, T. Dandekar, K. Becker, S. Gromer, *Antimicrob. Agents Chemother.* **2008**, *52*, 183–191.
- G. N. Sarma, S. N. Savvides, K. Becker, M. Schirmer, R. H. Schirmer, P. A. Karplus, *J. Mol. Biol.* **2003**, *328*, 893–907.
- T. Akompong, N. Ghori, K. Haldar, *Antimicrob. Agents Chemother.* **2000**, *44*, 88–96.
- G. Eberlein, T. C. Bruice, *J. Am. Chem. Soc.* **1983**, *105*, 6685–6697.
- A. Mattevi, *Trends Biochem. Sci.* **2006**, *31*, 276–283.
- a) V. I. Carrara, J. Zwang, E. A. Ashley, R. N. Price, K. Stepniewska, M. Barends, A. Brockman, T. Anderson, R. McGready, L. Phaiphun, S. Proux, M. van Vugt, R. Hutagalung, K. M. Lwin, A. P. Phyto, P. Preechapornkul, M. Imwong, S. Pukrittayakamee, P. Singhasivanon, N. J. White, F. Nosten, *PLoS ONE* **2009**, *4*, e4551; b) A. M. Dondorp, S. Yeung, L. White, C. Nguon, N. P. J. Day, D. Socheat, L. von Seidlein, *Nat. Rev. Microbiol.* **2010**, *8*, 272–280.
- M. Enserink, *Science* **2010**, *328*, 845–846.
- a) Z. I. Cabantchik, O. Kakhlon, S. Epsztejn, G. Zanninelli, W. Breuer, "Intracellular and Extracellular Labile Iron Pools" in *Iron Chelation Therapy* (Ed.: C. Hershko), Kluwer Academic, New York, **2002**, pp. 55–75; b) H. Boukhalfa, A. L. Crumbliss, *Biomaterials* **2002**, *15*, 325–339; c) O. Kakhlon, Z. I. Cabantchik, *Free Radical Biol. Med.* **2002**, *33*, 1037–1046; d) S. C. Andrews, A. K. Robertson, F. Rodriguez-Quinones, *FEMS Microbiol. Rev.* **2003**, *27*, 215–237; e) P. F. Scholl, A. K. Tripathi, D. J. Sullivan, *Curr. Top. Microbiol. Immunol.* **2005**, *295*, 293–324.
- S. Mowry, P. Ogren, *J. Chem. Educ.* **1999**, *76*, 970–973.
- A. J. Hallcock, E. S. F. Berman, R. N. Zare, *J. Am. Chem. Soc.* **2003**, *125*, 1158–1159.
- H. Görner, *Photochem. Photobiol. Sci.* **2008**, *7*, 371–376.
- J. F. J. Engbersen, A. Koudjijis, H. C. van der Plas, *Recl. Trav. Chim. Pays-Bas* **1986**, *105*, 494–502.
- R. K. Haynes, H.-W. Chan, C.-M. Lung, N.-C. Ng, H.-N. Wong, L. Y. Shek, I. D. Williams, M. F. Gomes, A. Cartwright, *ChemMedChem* **2007**, *2*, 1448–1463.
- D. J. T. Porter, G. Blankenhorn, L. L. Ingraham, *Biochem. Biophys. Res. Commun.* **1973**, *52*, 447–452.
- L. G. Lee, G. M. Whitesides, *J. Am. Chem. Soc.* **1985**, *107*, 6999–7008.
- J. K. Baker, J. D. McChesney, H. T. Chi, *Pharm. Res.* **1993**, *10*, 662–666.
- C. W. Jefford, U. Burger, P. Millasson-Schmidt, G. Bernadinelli, B. L. Robinson, W. Peters, *Helv. Chim. Acta* **2000**, *83*, 1239–1246.

- [41] C. C. Böhme, L. D. Arscott, K. Becker, R. H. Schirmer, C. H. Williams, *J. Biol. Chem.* **2000**, *275*, 37317–37323.
- [42] N. Vyas, B. A. Avery, M. A. Avery, C. M. Wyandt, *Antimicrob. Agents Chemother.* **2002**, *46*, 105–109.
- [43] W. Buckel, B. T. Golding, *Ann. Rev. Microbiol.* **2006**, *60* 27–49.
- [44] A. E. Mercer, J. L. Maggs, X.-M. Sun, G. M. Cohen, J. Chadwick, P. M. O'Neill, B. K. Park, *J. Biol. Chem.* **2007**, *282*, 9372–9382.
- [45] S. Sollner, S. Deller, P. Macheroux, P. A. Palfey, *Biochemistry* **2009**, *48*, 8636–8643.
- [46] Y. T. Lee, J. F. A. Fisher, *Bioorg. Chem.* **2000**, *28*, 163–175.
- [47] G. H. Posner, D. Wang, J. N. Cumming, C. H. Oh, A. N. French, A. L. Bodley, T. A. Shapiro, *J. Med. Chem.* **1995**, *38*, 2273–2275.
- [48] R. K. Haynes, H.-N. Wong, K. W. Lee, C.-M. Lung, L.-Y. Shek, I. D. Williams, S. L. Croft, L. Vivas, L. Rattray, L. Stewart, *ChemMedChem* **2007**, *2*, 1464–1479.
- [49] M. A. Avery, P.-C. Fan, J. M. Karle, J. D. Bonk, R. Miller, D. K. Goins, *J. Med. Chem.* **1996**, *39*, 1885–1897.
- [50] P. L. Olliaro, R. K. Haynes, B. Meunier, Y. Yuthavong, *Trends Parasitol.* **2001**, *17*, 121–126.
- [51] a) M. A. Avery, W. K. M. Chong, J. E. Bupp, *J. Chem. Soc. Chem. Commun.* **1990**, 1487–1489; b) M. A. Avery, F. Gao, W. K. M. Chong, T. F. Hendrickson, W. D. Inman, P. Crews, *Tetrahedron* **1994**, *50*, 952–957.
- [52] a) S. Krishna, A.-C. Uhlemann, R. K. Haynes, *Drug Resist. Updates* **2004**, *7*, 233–244; b) R. K. Haynes, S. Krishna, *Microbes Infect.* **2004**, *6*, 1339–1346.
- [53] A. K. O. Boubacar, S. Pethe, J.-P. Mahy, F. Lederer, *Biochemistry* **2007**, *46*, 13080–13088.
- [54] a) A. O. Cuello, C. M. McIntosh, V. M. Rotello, *J. Am. Chem. Soc.* **2000**, *122*, 3517–3521; b) A. J. Goodman, E. C. Breinlinger, C. M. McIntosh, L. N. Grimaldi, V. M. Rotello, *Org. Lett.* **2001**, *3*, 1531–1534.
- [55] C. Morin, T. Besset, J.-C. Moutet, M. Fayolle, M. Brückner, D. Limosin, K. Becker, E. Davioud-Charvet, *Org. Biomol. Chem.* **2008**, *6*, 2731–2742.
- [56] F. C. Chang, R. P. Swenson, *Biochemistry* **1997**, *36*, 9013–9021.
- [57] R. L. Krauth-Siegel, H. Bauer, R. H. Schirmer, *Angew. Chem.* **2005**, *117*, 698–724; *Angew. Chem. Int. Ed.* **2005**, *44*, 690–715.
- [58] A report indicates a pathway to increased tolerance by a quiescence mechanism induced through drug pressure, arresting parasite development at the ring stage. The genetic basis for this effect remains to be determined, but clearly, this cannot be associated with acquisition of resistance per se: B. Witkowski, J. Lelièvre, M. J. L. Barragán, V. Laurent, X.-Z. Su, A. Berry, F. Benoit-Vical, *Antimicrob. Agents Chemother.* **2010**, *54*, 1872–1877.
- [59] J. L. Vennerstrom, J. W. Eaton, *J. Med. Chem.* **1988**, *31*, 1269–1277.
- [60] S. Krishna, L. Bustamante, R. K. Haynes, H. M. Staines, *Trends Pharmacol. Sci.* **2008**, *29*, 520–527.
- [61] S. Uriq, K. Becker, *Semin. Cancer Biol.* **2006**, *16*, 452–465.
- [62] S. Danson, T. H. Ward, J. Butler, M. Ranson, *Cancer Treat. Rev.* **2004**, *30*, 437–449.
- [63] J. Lutz, F. Hollmann, T. V. Ho, A. Schnyder, R. H. Fish, A. Schmid, *J. Organomet. Chem.* **2004**, *689*, 4783–4790.
- [64] J.-M. Liu, M.-Y. Ni, J.-F. Fan, Y.-Y. Tu, Z.-H. Wu, Y.-L. Wu, W.-S. Zhou, *Acta Chimica Sinica* **1979**, *37*, 129–141.

Received: May 26, 2010

Revised: June 7, 2010

Published online on July 13, 2010